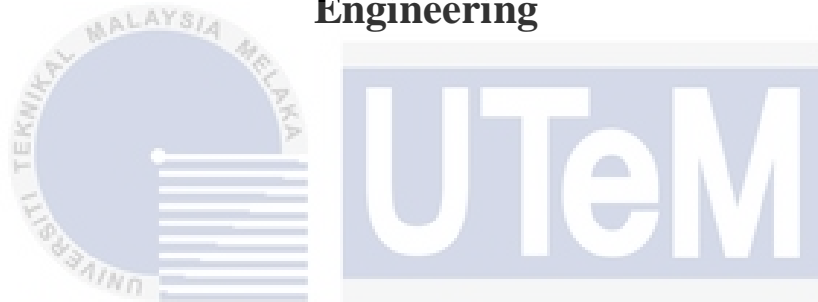




**Faculty of Electronics and Computer Technology and  
Engineering**



**MICROFIBRE DOUBLE LOOP RESONATOR FOR HUMIDITY  
SENSOR**

UNIVERSITI TEKNIKAL MALAYSIA MELAKA

**HUANG CERISE**

**Bachelor of Electronics Engineering Technology (Telecommunications) with Honours**

**2024**

# **MICROFIBRE DOUBLE LOOP RESONATOR FOR HUMIDITY SENSOR**

**HUANG CERISE**

**A project report submitted  
in partial fulfillment of the requirements for the degree of  
Bachelor of Electronics Engineering Technology (Telecommunications) with Honours**



**Faculty of Electrical and Electronic Engineering Technology**

اويورسي تي بيكيكل مليسيا ملاك

UNIVERSITI TEKNIKAL MALAYSIA MELAKA

**UNIVERSITI TEKNIKAL MALAYSIA MELAKA**

**2024**

**BORANG PENGESAHAN STATUS LAPORAN  
PROJEK SARJANA MUDA II**

Tajuk Projek : Microfibre Double Loop Resonator for Humidity Sensor

Sesi Pengajian : 2023/2024

Saya Huang Cerise mengaku membenarkan laporan Projek Sarjana

Muda ini disimpan di Perpustakaan dengan syarat-syarat kegunaan seperti berikut:

1. Laporan adalah hakmilik Universiti Teknikal Malaysia Melaka.
2. Perpustakaan dibenarkan membuat salinan untuk tujuan pengajian sahaja.
3. Perpustakaan dibenarkan membuat salinan laporan ini sebagai bahan pertukaran antara institusi pengajian tinggi.
4. Sila tandakan (✓):

**SULIT\***

(Mengandungi maklumat yang berdarjah keselamatan atau kepentingan Malaysia seperti yang termaktub di dalam AKTA RAHSIA RASMI 1972)

(Mengandungi maklumat terhad yang telah ditentukan oleh organisasi/badan di mana penyelidikan dijalankan)

/

**TIDAK TERHAD**

Disahkan oleh:



(TANDATANGAN PENULIS)

Alamat Tetap:

**DR. MD ASHAF BIN MD JOHARI**

Pensyarah Kanan

(GOP DAN TANDATANGAN PENYELIA)

Fakulti Teknologi dan Kejuruteraan Elektrik dan Elektronik (FTKEK)  
Universiti Teknikal Malaysia Melaka (UTeM)

Tarikh: 13 / 1 / 2024

Tarikh: 19 / 1 / 2024

## DECLARATION

I declare that this project report entitled “Microfibre Double Loop Resonator for Humidity Sensor” is the result of my own research except as cited in the references. The project report has not been accepted for any degree and is not concurrently submitted in candidature of any other degree.

Signature

:



Student Name

:

HUANG CERISE

Date

:

13 / 1 / 2024



## APPROVAL

I hereby declare that I have checked this project report and in my opinion, this project report is adequate in terms of scope and quality for the award of the degree of Bachelor of Electrical Engineering Technology with Honours.

Signature :



Supervisor Name : DR. MD ASHADI BIN MD JOHARI

Date : 19 / 1 / 2024



## DEDICATION

*To my beloved mother, Liew Phoy Yun, and father, Victor Huang Jiunn Yeh,*

*And to my kind lecturers*

*For their*

*Love, sacrifice, encouragement, and best wishes*

*Along with my hardworking and respected Supervisor*

*Dr. Md Ashadi bin Md Johari*



## ABSTRACT

Reliable humidity readings are critical in a variety of industries, including agriculture. Fibre optic sensors have several advantages over electronic sensors, and much research has been conducted on this topic in recent years. The development of optical structures for determining humidity, as well as the development of novel materials for this purpose has been investigated. A double loop fibre optic humidity sensor is being developed as part of a research project. As a result, a good humidity sensor from the microfibre double loop resonator is developed.



## ***ABSTRAK***

Bacaan kelembapan yang boleh dipercayai adalah kritikal dalam pelbagai industri, termasuk pertanian. Penderia gentian optik mempunyai beberapa kelebihan berbanding penderia elektronik, dan banyak penyelidikan telah dijalankan mengenai topik ini dalam beberapa tahun kebelakangan ini. Pembangunan struktur optik untuk menentukan kelembapan, serta pembangunan bahan baru untuk tujuan ini telah disiasat. Sensor kelembapan gentian optik gelung berganda sedang dibangunkan sebagai sebahagian daripada projek penyelidikan. Hasilnya, penderia kelembapan yang baik daripada resonator gelung berganda mikrofiber dibangunkan.



## ACKNOWLEDGEMENTS

First and foremost, I would like to express my gratitude to my supervisor, Dr. Md Ashadi bin Md Johari for his precious guidance, words of wisdom and patient throughout this project.

I am also indebted to Universiti Teknikal Malaysia Melaka (UTeM) for the financial support which enables me to accomplish the project.

My highest appreciation goes to my parents and family members for their love and prayer during the period of my study.

Finally, I would like to thank all the staffs and classmates, the Faculty members, as well as other individuals who are not listed here for being co-operative and helpful.



## TABLE OF CONTENTS

	<b>PAGE</b>
<b>DECLARATION</b>	
<b>APPROVAL</b>	
<b>DEDICATIONS</b>	
<b>ABSTRACT</b>	<b>i</b>
<b>ABSTRAK</b>	<b>ii</b>
<b>ACKNOWLEDGEMENTS</b>	<b>iii</b>
<b>TABLE OF CONTENTS</b>	<b>i</b>
<b>LIST OF TABLES</b>	<b>iv</b>
<b>LIST OF SYMBOLS</b>	<b>viii</b>
<b>LIST OF ABBREVIATIONS</b>	<b>ix</b>
<b>LIST OF APPENDICES</b>	<b>x</b>
<b>CHAPTER 1 INTRODUCTION</b>	<b>1</b>
1.1 Background	1
1.2 Problem Statement	2
1.3 Project Objective	3
1.4 Scope of Project	3
<b>CHAPTER 2 LITERATURE REVIEW</b>	<b>4</b>
2.1 Introduction	4
2.2 Fibre Optic	4
2.2.1 Single Mode	5
2.2.2 Multimode	6
2.3 Propagation of Light Among Fibre	6
2.3.1 Reflective and Reflective index	7
2.3.2 Numerical Aperture	7
2.4 Various Shapes and Sizes of Fibre Optic Sensor	9
2.4.1 Fibre Optic Shape Sensor (FOSS)	9
2.4.1.1 Shape Sensing Based on Optical Fibre Sensors	9
2.4.1.2 Strain Sensing Technology	10
2.4.1.3 Application of FOSS	11
2.4.2 Optical Fibre Humidity Sensors (OFHS)	11
2.4.2.1 Optical Absorption Sensors	12
2.4.2.2 Modal Interferometers	12
2.4.2.3 Resonators and Whispering Galleries Modes	13

2.4.2.4	Optical Fibre Humidity Sensors Based on Lossy Mode Resonances	13
2.4.3	Fibre Bragg Grating (FBG)	14
2.4.3.1	FBG Sensor Grating Profiles	14
2.4.3.2	Etching of FBG	15
2.4.3.3	Coating of FBG	16
2.4.4	Polymer Optical Fibre Sensor (POFs)	17
2.4.4.1	Principle of Operation and Simulations	17
2.4.4.2	Sensor Measurements	18
2.5	Advantages and Disadvantages of Fibre Optics	19
2.6	Journal Comparison from Previous Work Related to the Project	20
2.7	Summary	22
<b>CHAPTER 3 METHODOLOGY</b>		<b>23</b>
3.1	Introduction	23
3.2	Project Flow	28
3.3	Procedure	29
3.3.1	Setting up Experiment with Fibre Optic Sensors	32
3.3.2	Stripping Process	33
3.3.3	Cleaning Process	34
3.3.4	Cleaving Process	35
3.3.5	Splicing Process	36
3.3.6	Tapering Process	37
3.3.7	Looping Process	38
3.3.8	Final Check on Fibre	39
3.3.9	Measuring of Fibre	40
3.4	Characterization of Fibre Optic Loop Sensor	41
3.4.1	Connector Inspection	41
3.4.2	Insertion Loss Test	42
3.4.3	Reflectance and Return Loss Test	42
3.4.4	Polarization Mode Dispersion	43
3.5	Summary	43
<b>CHAPTER 4 RESULTS AND DISCUSSIONS</b>		<b>44</b>
4.1	Introduction	44
4.2	Size of Microfibre Optical Loop Sensor	44
4.3	Result and Analysis for Humidity over Time using Calcium Chloride	45
4.3.1	Single Loop Resonator	45
4.3.1.1	100% of Humidity (0 pieces of Calcium Chloride) Tested on 1310nm and 1550nm Wavelengths	46
4.3.1.2	90% of Humidity (1 piece of Calcium Chloride) Tested on 1310nm and 1550nm Wavelengths	47
4.3.1.3	80% of Humidity (2 pieces of Calcium Chloride) Tested on 1310nm and 1550nm Wavelengths	48
4.3.1.4	70% of Humidity (3 pieces of Calcium Chloride) Tested on 1310nm and 1550nm Wavelengths	49
4.3.1.5	60% of Humidity (4 pieces of Calcium Chloride) Tested on 1310nm and 1550nm Wavelengths	50

4.3.1.6	50% of Humidity (5 pieces of Calcium Chloride) Tested on 1310nm and 1550nm Wavelengths	51
4.3.1.7	Comparison	52
4.3.2	Double Loop Resonator	53
4.3.2.1	100% of Humidity (0 pieces of Calcium Chloride) Tested on 1310nm and 1550nm Wavelengths	53
4.3.2.2	90% of Humidity (1 piece of Calcium Chloride) Tested on 1310nm and 1550nm Wavelengths	54
4.3.2.3	80% of Humidity (2 pieces of Calcium Chloride) Tested on 1310nm and 1550nm Wavelengths	55
4.3.2.4	70% of Humidity (3 pieces of Calcium Chloride) Tested on 1310nm and 1550nm Wavelengths	56
4.3.2.5	60% of Humidity (4 pieces of Calcium Chloride) Tested on 1310nm and 1550nm Wavelengths	57
4.3.2.6	50% of Humidity (5 pieces of Calcium Chloride) Tested on 1310nm and 1550nm Wavelengths	58
4.3.2.7	Comparison	59
4.4	Analysis of Results of the Average of Microfibre Interaction with Power over Humidity	60
4.4.1	Comparison of Average Power of Single and Double Loop Resonator for Different Levels of Humidity for 1310nm	60
4.4.2	Comparison of Average Power of Single and Double Loop Resonator for Different Levels of humidity for 1550nm	61
4.4.3	Comparison of Average Power of 1310nm and 1550nm Wavelengths for Single Loop at Different Levels of Humidity	62
4.4.4	Comparison of Average Power of 1310nm and 1550nm Wavelengths for Double Loop for Different Levels of Humidity	63
<b>CHAPTER 5 CONCLUSION AND RECOMMENDATIONS</b>		<b>64</b>
5.1	Conclusion	64
5.2	Suggestion for Future Works	65
<b>REFERENCES</b>		<b>66</b>
<b>APPENDICES</b>		<b>69</b>

## LIST OF TABLES

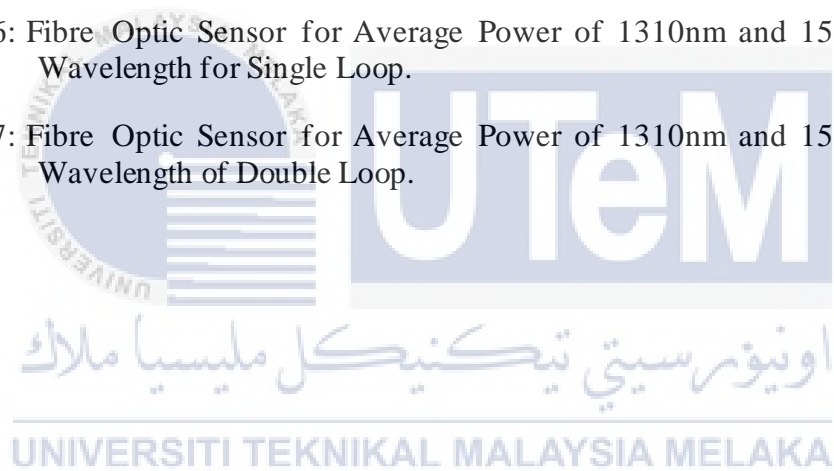
<b>TABLE</b>	<b>TITLE</b>	<b>PAGE</b>
Table 2.1:	Journal Comparison	20
Table 4.1:	Recorded Data for 100% Humidity	46
Table 4.2:	Recorded Data for 90% Humidity	47
Table 4.3:	Recorded Data for 80% Humidity	48
Table 4.4:	Recorded Data for 70% Humidity	49
Table 4.5:	Recorded Data for 60% Humidity	50
Table 4.6:	Recorded Data for 50% Humidity	51
Table 4.7:	Recorded Data for Comparison of Humidity (%) and 1310nm and 1550nm Wavelengths for Single Loop Resonator	52
Table 4.8:	Recorded Data for 100% Humidity	53
Table 4.9:	Recorded Data for 90% Humidity	54
Table 4.10:	Recorded Data for 80% Humidity	55
Table 4.11:	Recorded Data for 70% Humidity	56
Table 4.12:	Recorded Data for 60% Humidity	57
Table 4.13:	Recorded Data for 50% Humidity	58
Table 4.14:	Recorded Data for Comparison of Humidity (%) and 1310nm and 1550nm Wavelengths for Double Loop Resonator	59
Table 4.15:	Recorded Data for Comparison of Average Power (dBm) and Humidity (%) of Single and Double Loop resonator at 1310nm	60
Table 4.16:	Recorded Data for Comparison of Average Power (dBm) and Humidity (%) of Single and Double Loop resonator at 1550nm	61
Table 4.17:	Recorded Data for Comparison of Average Power (dBm) and Humidity (%) of 1310nm and 1550nm	62
Table 4.18:	Recorded Data for Comparison of Average Power (dBm) and Humidity (%) of 1310nm and 1550nm	63

## LIST OF FIGURES

<b>FIGURE</b>	<b>TITLE</b>	<b>PAGE</b>
Figure 1.1:	Snell's Law Model	2
Figure 2.1:	Basic Structure of Optical Fibre	4
Figure 2.2:	Dispersion of Common Types of Single-Mode Fibre [4]	5
Figure 2.3:	Different Types of Fibres [5]	6
Figure 2.4:	The acceptance cone and propagation of light in an optical fibre	7
Figure 2.5:	Numerical Aperture (NA) angle	8
Figure 2.6:	Demonstration of Snell's Law [8]	8
Figure 2.7:	Historical progress in FOSS	10
Figure 2.8:	Classification of optical fibre humidity sensors	11
Figure 2.9:	Various grating profiles of FBG	14
Figure 2.10:	(a) Longitudinal section of the coupling (and sensing) area of the POF liquid sensor. (b) POF liquid sensor. (c) One arm sensor fibre after polishing	18
Figure 2.11:	POF sensor set-up to determine liquid level in tanks [12]	18
Figure 3.1:	A pair of SC/UPC connectors for Single Mode Fibre Pigtaills	23
Figure 3.2:	The Cutter to cut fibre optic cables	24
Figure 3.3:	The stripper to remove the outer jacket or coating of fibre optic cables	24
Figure 3.4:	Cleaning tool used after stripping fibre optic cables	25
Figure 3.5:	Fujikura Hand Cleaver used to cut the fibre tips to the proper length for splicing	25
Figure 3.6:	Fusion splicer machine which splits two fibres together automatically	26
Figure 3.7:	Calcium Chloride used for this experiment.	26
Figure 3.8:	Light source that transmits wavelength of 1310nm and 1550nm light.	27
Figure 3.9:	Pulsed laser light flowing via an optical fibre is transmitted and analysed during OTDR testing.	27

Figure 3.10: The project flow of this report	28
Figure 3.11: The flowchart of stripping, cleaning and cleaving the fibre optic cable	29
Figure 3.12: The flowchart of splicing, tapering and looping the fibre optic cable.	30
Figure 3.13: The flowchart of conducting the experiment in developing fibre optic as a sensor.	31
Figure 3.14: The setup of the equipment.	32
Figure 3.15: The process of stripping the fibre optic cable.	33
Figure 3.16: The process of cleaning the stripped fibre optic cable.	34
Figure 3.17: The process of cleaving the fibre optic cable.	35
Figure 3.18: The process of splicing the fibre optic cable.	36
Figure 3.19: The process of tapering the fibre optic cable.	37
Figure 3.20: The process of looping the fibre optic cable.	38
Figure 3.21: The process of testing fibre connection using laser.	39
Figure 3.22: The process of measuring humidity.	40
Figure 3.23: The process of measuring humidity of single loop (left) and double loop (right) resonator.	40
Figure 3.24: Cleaning kit for connectors.	41
Figure 3.25: 0dB reference at power meter then to test the insertion loss.	42
Figure 3.26: Return loss testing.	42
Figure 3.27: Three types of dispersion in fibre optics.	43
Figure 4.1: New Size of the Microfibre optic sensor (right).	44
Figure 4.2: Microfiber Optic Single Loop Sensor at 100% Humidity.	46
Figure 4.3: Microfiber Optic Single Loop Sensor at 90% Humidity.	47
Figure 4.4: Microfiber Optic Single Loop Sensor at 80% Humidity.	48
Figure 4.5: Microfiber Optic Single Loop Sensor at 70% Humidity.	49
Figure 4.6: Microfiber Optic Single Loop Sensor at 60% Humidity.	50
Figure 4.7: Microfiber Optic Single Loop Sensor at 50% Humidity.	51

Figure 4.8: Microfiber Optic Single Loop Sensor at 100% Humidity.	53
Figure 4.9: Microfiber Optic Single Loop Sensor at 90% Humidity.	54
Figure 4.10: Microfiber Optic Single Loop Sensor at 80% Humidity.	55
Figure 4.11: Microfiber Optic Single Loop Sensor at 70% Humidity.	56
Figure 4.12: Microfiber Optic Single Loop Sensor at 60% Humidity.	57
Figure 4.13: Microfiber Optic Single Loop Sensor at 50% Humidity.	58
Figure 4.14: Fibre Optic Sensor for Average Power of Single and Double Loop of 1310nm.	60
Figure 4.15: Fibre Optic Sensor for Average Power of Single and Double Loop of 1550nm.	61
Figure 4.16: Fibre Optic Sensor for Average Power of 1310nm and 1550nm Wavelength for Single Loop.	62
Figure 4.17: Fibre Optic Sensor for Average Power of 1310nm and 1550nm Wavelength of Double Loop.	63



## LIST OF SYMBOLS

$\theta_1$	-	Incident angle
$\theta_2$	-	Refracted angle
$n_2$	-	Refractive indices of material 2
$n_1$	-	Refractive indices of material 1
NA	-	Numerical Aperture
$n$	-	Refraction indeks of the medium
$\Theta$	-	Half-angle of the maximum core
$\lambda$	-	Wavelength
$B$	-	Bragg
$\Lambda$	-	Grating period
$\varepsilon$	-	Fibre polishing depth



## LIST OF ABBREVIATIONS

FBG	-	Fibre Bragg Gratings
FPI	-	Fabry-Perot Interferometers
DFOS	-	Distributed Fiber Optic Sensors
NDSF	-	Non-Dispersion-Shifted Fibre
DSF	-	Dispersion-Shifted Fibre
NZ-DSF	-	Non-Zero Dispersion-Shifted Fibre
FOSS	-	Fibre Optic Shape Sensor
OFS	-	Optical Fibre Sensor
EM	-	Electromagnetic
OFHS	-	Optical Fibre Humidity Sensor
PCS	-	Plastic-Cladding Silica
POF	-	Plastic Optical Fibre
PCF	-	Photonic Crystal Fibre
NATOF	-	Non-Adiabatic Tapered Optical Fibre
SMF	-	Single-Mode Fibre
LMR	-	Lossy Mode Resonance
SPR	-	Surface Plasmon Resonance
TM	-	Transverse Magnetic
TE	-	Transverse Electric
LSPR	-	Localised Surface Plasmon Resonance
OF	-	Optical Fibre
ASE	-	Amplified Spontaneous Emitter
OTDR	-	Optical Time Domain Reflectometer

UNIVERSITI TEKNIKAL MALAYSIA MELAKA

## LIST OF APPENDICES

APPENDIX	TITLE	PAGE
Appendix A	Gantt Chart for PSM1	69
Appendix B	Gantt Chart for PSM2	70



# CHAPTER 1

## INTRODUCTION

### 1.1 Background

Optical microfiber is a type of optical waveguide with a diameter that is usually in 10 micrometers made of glass or other materials. The microfiber is typically a long and thin strand of glass that can range in length from several millimeters to hundreds of micrometers. The applications for optical microfibers include optical sensing, nonlinear optics and telecommunications. They can also be used with other devices such as microfluidic channels and used to create compact sensors with high sensitivity due to their small size and flexibility. There are two types of fiber optics which are single-mode fibers that is used for long-distance communication and multimode fibers which are used to short-distance communication.

Optical fibre uses Snell's Law which is also known as the law of refraction. It describes how light behaves when it passes through the interface of two materials with different refractive indices. Snell's Law states that the ratio of sine of incident and refracted angle is equal to the ratio of the refractive index of the materials at the interface.

$$\frac{\sin \theta_1}{\sin \theta_2} = \frac{n_2}{n_1}$$

$\theta_1$  = incident angle

$\theta_2$  = refracted angle

$n_2$  = refractive indices of material 2

$n_1$  = refractive indices of material 1

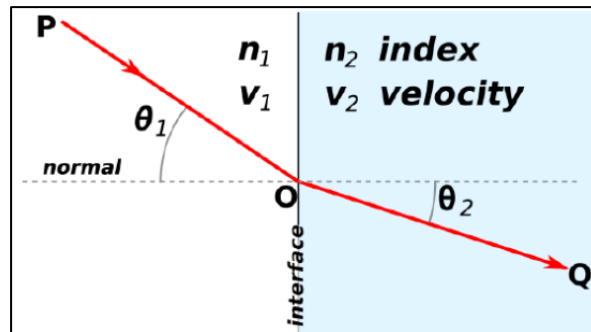


Figure 1.1: Snell's Law Model

This project aims to create a microfiber double loop resonator for humidity sensor for use in agricultural industry specifically in greenhouses to adjust the humidity and optimize crop production. The humidity sensor is essential for optimal growth conditions and to prevent plant stress such as waterlogging or dehydration. The humidity sensors can detect problems early and save energy and cost. Overall, this study aims to investigate the impact of fiber loop on bending fibre which leads to increasing the sensitivity of the sensor.

## 1.2 Problem Statement

In the agricultural industry, sensor development is crucial to optimize production. To achieve optimal plant growth, the farming industry has established that temperature and air moisture are essential factors and changes in relative humidity can have severe consequences for the crops. High humidity levels and poor ventilation in the greenhouse contributes to pests and diseases which lowers crop yield and quality. Hence, improved ventilation and good environmental monitoring can prevent such issues from happening. Fibre optic sensors are used throughout this research to measure air moisture in the greenhouse which is beneficial in the agricultural sector. These sensors which comes in various forms and sizes are designed to keep track of a wide range of environmental factors such as humidity, light, temperature and more in order to support famers in optimizing crop growth and yield.

### 1.3 Project Objective

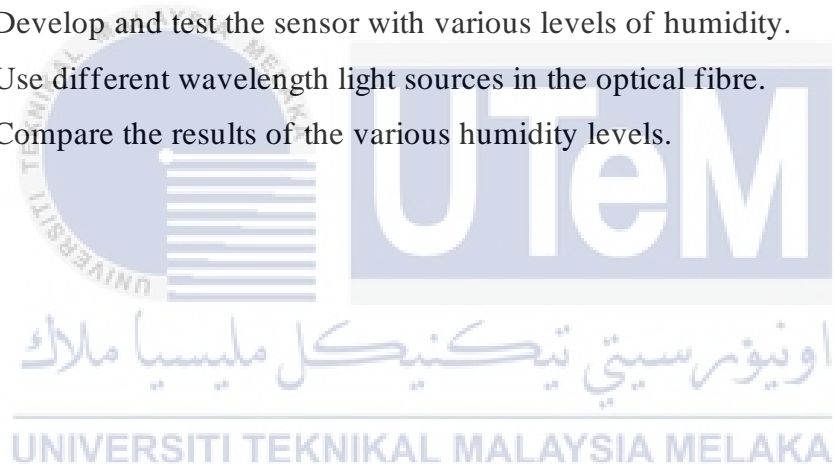
The main aim of this project is to develop an effective and suitable method for accurately evaluating system-wide humidity sensors by using the optical loop fiber distribution network. Specifically, the objectives are as follows:

- a) To understand the literature of Optical Microfiber double loop resonator.
- b) To develop Optical Microfiber Loop resonator for humidity sensor.
- c) To analyze the performance of the humidity sensor using Optical Microfiber Loop with various humidity levels.

### 1.4 Scope of Project

The scope of this project are as follows:

- a) Develop and test the sensor with various levels of humidity.
- b) Use different wavelength light sources in the optical fibre.
- c) Compare the results of the various humidity levels.



## CHAPTER 2

### LITERATURE REVIEW

#### 2.1 Introduction

This part covered the entire project's literature review and the project development. The additional materials used for this project are journals, articles and books from previous work related to the project's topic that would serve as primary sources. This chapter will cover everything from the fundamentals to related research application. This stage is important to know the concept of fibre optics and how they work before the next step which is to develop a Microfibre Double Loop Resonator for Humidity Sensor.

#### 2.2 Fibre Optic

Since fibre optic is versatile and may be bundled as connections, fibre optics can be employed as a medium for telecommunications organizations. Since a light travels through a fibre with little fading, it is advantageous for long-distance communication over electrical connections. In order to spread out long separations, a pair of repeaters can be used. The use of measurements is essential in a variety of industries, including those that produce food, monitor the environment, process chemicals, and perform medical diagnostics. [1]

A fibre optic cable consists of thin glass fibre that is usually made of fused silica ( $\text{SiO}_2$ ) that is enclosed by a polymer or metal layers that protect it. [2]

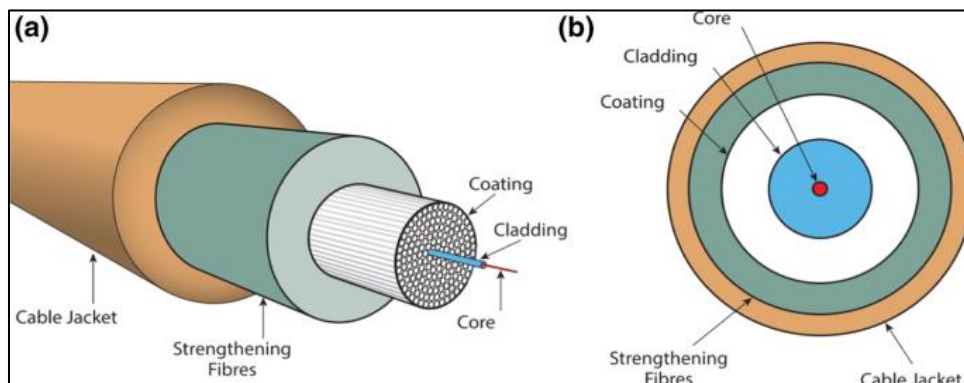


Figure 2.1: Basic Structure of Optical Fibre

A single thin optic fibre consists of three primary components, the core, the cladding and the coating or buffer. Then a cable jacket and strengthening fibres are placed around it. A cylindrical rod of a dielectric material is the very thin core in the centre of the fibre, with a diameter that ranges from 8 to 63  $\mu\text{m}$ . [3]

### 2.2.1 Single Mode

There are three basic classes of single-mode fibre that are used in telecommunication system. The Non-DSF (Non-Dispersion-Shifted-Fibre) type is the oldest and is still the most frequently used. It is tuned for 1310 nm operation, and later, 1550 nm systems were introduced. The maximum transmission rate and distance are constrained by the high dispersion at that wavelength. Then DSF (Dispersion-Shifted Fibre), which operates at 1550nm, was introduced. When multiple, closely spaced wavelengths in the 1550 nm band were transmitted as in DWDM systems, it exhibited severe nonlinearities. The last type is NZ-DSF (non-zero dispersion-shifted fibre), which comes in positive and negative dispersion varieties.

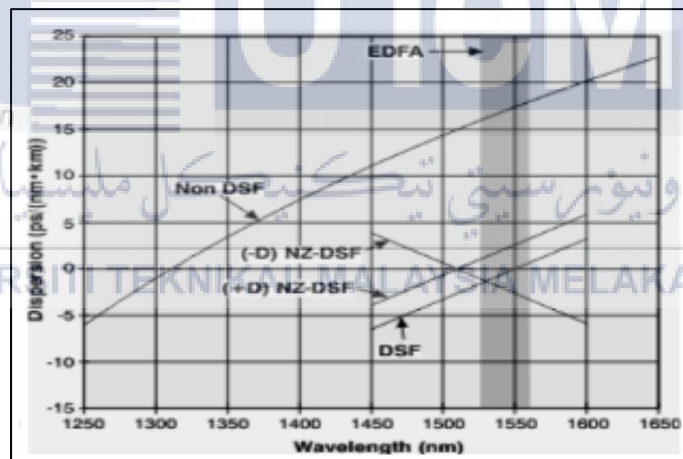


Figure 2.2: Dispersion of Common Types of Single-Mode Fibre [4]

In comparison to multimode fibre, single mode step-index fibre has a central core diameter that ranges from 8 to 12  $\mu\text{m}$ . Light rays that enter the fibre either travel all the way to the core or are only briefly reflected. [5]

## 2.2.2 Multimode

It has a larger core diameter and relative refractive index than single mode fibre and allows light rays to travel through a large number of modes. Multimode also comes in two types which are Multimode Step-Index Fibre and Multimode Graded-Index Fibre. [5]

Multimode Step-Index fibre's core have a constant refractive index throughout, changing suddenly or in a step pattern at the core-cladding boundary. More light can be coupled into the fibre thanks to the 100um core size, which is larger. Consequently, there may be increased signal loss and distortion. [6]

Multimode Graded-Index Fibre is a multimode step index with lower signal loss and distortion. The core's refractive index is changed in a parabolic fashion so that the maximum refractive index is at the core's centre (50 or 62.5um). [5]

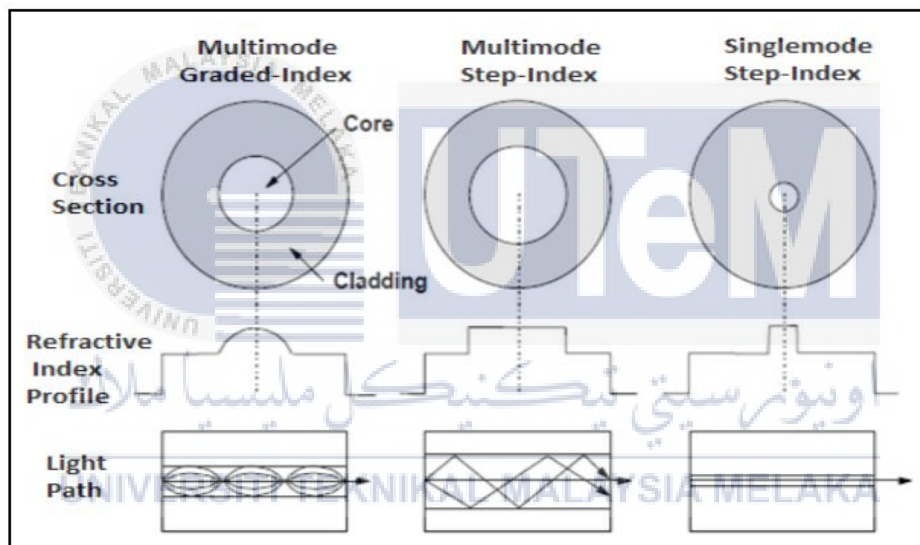


Figure 2.3: Different Types of Fibres [5]

## 2.3 Propagation of Light Among Fibre

In fibre optics, the information carrier is a light beam that travels at the speed of light ( $3 \times 10^8$  m/s), which is much faster and more effective than electronic devices that use electric current. The light that is pumped into the core of the optical fibre propagates across the core-to-cladding barrier. Since the cladding is made of a material with a higher refractive index than the core, light will continue to travel along the cable. [7]

### 2.3.1 Reflective and Reflective index

The core of an optical fibre waveguide is a single solid electric cylinder with a refractive index of refraction of  $n_1$ . The core is surrounded by cladding, which is a solid dielectric with a refractive index less than  $n_1$ . Variations in the material composition of the core result in two common types of fibres. Step index fibres have a constant refractive index throughout the core and a sudden (step) change at the cladding. When the refractive index of the core varies with radial distance from the centre, the fibre is referred to as graded index fibre. A light beam is incident within the acceptance cone semi-angle of the fibre, which is dependent on the refractive index of the fibre's core and cladding, the beam of light can propagate along the length of a cylindrical waveguide. The incident angle of the light into the fibre should be such that the internal reflection angle is greater than the critical angle. Total internal reflection will keep the light inside the fibre and allow it to travel to the far end. Light will seep into the cladding if the requirement is not met.

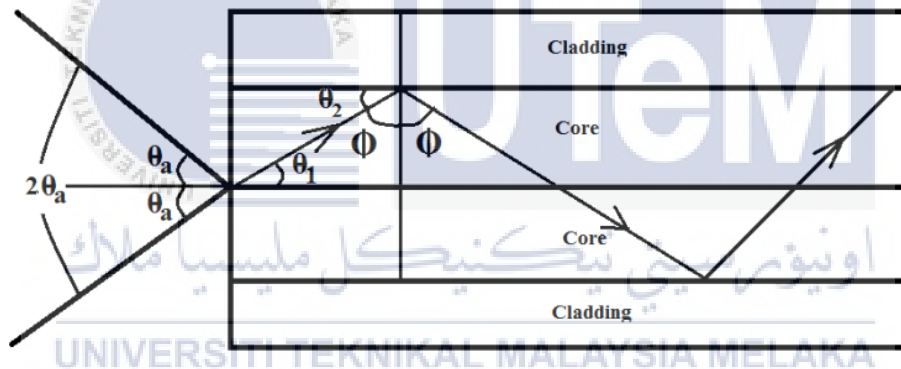


Figure 2.4: The acceptance cone and propagation of light in an optical fibre

### 2.3.2 Numerical Aperture

A number with no dimensions that describes the range of angles at which the system can accept or emit light. NA has the property of remaining constant for a beam as it passes from one material to another when the index of refraction is included in its definition and there is no optical power at the interface. Different branches of optics define the term differently. In microscopy, numerical aperture is commonly used to describe an objective's acceptance cone (and thus its capacity for light collection and resolution) as well as the cone of light entering or leaving a fibre optic cable. The numerical aperture is the maximum angle

at which light incident on a fibre is completely internally reflected and can be properly transmitted along the fibre.

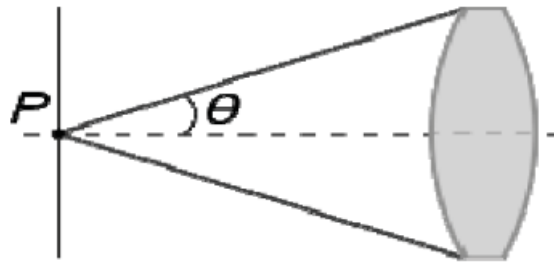


Figure 2.5: Numerical Aperture (NA) angle

An optical system's numerical numerical aperture is defined as  $NA = n \sin \theta$ , where  $n$  is the medium's refraction index and  $\theta$  is the half-angle of the maximum cone of light that can enter or exit. This is typically the angle of the system's actual marginal ray. Because the index of refraction is taken into account, the NA of a pencil of rays is an invariant as it moves from one material to another across a flat surface. This is easily demonstrated by rearranging Snell's law to discover that  $n \sin \theta$  is constant across an interface.

$$NA = \sqrt{n_1^2 - n_2^2}$$

Where  $n_1$  is the index of refraction of the first medium and  $n_2$  is the index of refraction of the second medium.

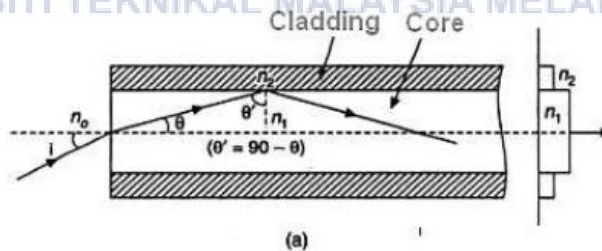


Figure 2.6: Demonstration of Snell's Law [8]

## **2.4 Various Shapes and Sizes of Fibre Optic Sensor**

The fibre optic sensors are increasingly being employed in the modern world to build machines and products that are beneficial and useful to humans. The fibre optic comes in many shapes and sizes which will be explained in Fibre Optic Shape Sensor (FOSS). This will be used in a variety of fields, including mechanical and aerospace engineering, civil engineering, biomedicine, and medicine, and will be an improvement over existing methods.

### **2.4.1 Fibre Optic Shape Sensor (FOSS)**

Fibre Optic Shape Sensor (FOSS) is defined as fibre optic cable with multiple cores and embedded strain sensors. The three-dimensional curvature in each instrumented portion is determined by simultaneously measuring strain in various cores, according to the following working principle. The longitudinal curvature function is calculated using interpolation or curve fitting from the strain values measured in the instrumented sections, and the shape is rebuilt using numerical integration of the curvature.

#### **2.4.1.1 Shape Sensing Based on Optical Fibre Sensors**

Shape sensors based on optical multicore fibres (a single fibre with multiple cores) and shape sensors based on multiple optical single-core fibres are the two main categories of FOSS. The distance between the sensor's axis and the outer cores. Other classifications can be made based on the number of cores or the strain sensing technology used, such as Fibre Bragg Grating (FBG), Rayleigh scattering, or Brillouin scattering. Existing shape sensing technologies include strain sensors, accelerometers, camera-based monitoring systems, RADAR or laser scanners, optoelectronic sensors, and fluoroscopy. Following that are Optical Fibre Sensors (OFS), which are used for continuous development of strain, temperature, moisture, vibrations, chemical agents, and other parameters..

### 2.4.1.2 Strain Sensing Technology

Strain Sensing Technology is divided into three phases which are strain sensing, curvature calculation and shape reconstruction. Fibre Bragg Gratings (FBG) are Bragg reflectors that have a long history of use as high-grade sensitive strain and temperature single-point sensors. The interaction between the atoms or molecules of a medium and the incident electromagnetic (EM) waves that pass through it causes light scattering, which consists of energy absorption and re-emission in different directions at different intensities. Light scatters via three distinct processes which are Raman (temperature sensitive), Brillouin (temperature and strain sensitive), and Rayleigh (temperature and strain sensitive). The historical progress in FOSS is shown below.

Historical progress in fiber optic shape sensing.

Starting year	Contribution	Description
1980s	Optical fiber strain sensors	Demonstration of distributed and quasi-distributed strain and temperature sensing using optical fibers.
1980s	Multiplexing technique	The development of multiplexing techniques to interrogate several Bragg grating sensors on a common fiber path enabled quasi-distributed measurements of strain and temperature.
- 1998	MCF-based interferometric bending sensor	The employment of optical multicore fiber enabled the measurement of degree and orientation of bending by comparing the strain in a pair of cores, using interferometric interrogation.
- 2000	Bending sensor using FBGs	Curvature measurements were demonstrated by using fiber Bragg gratings. The gratings were written into separate cores of a multicore fiber and acted as independent, but isothermal, strain gauges, providing a temperature-independent measurement of the local curvature.
- 2003	3D bend sensor	By employing three or more non-aligned strain sensors inscribed into the cores of an optical multicore fiber section, it was possible to measure the local three-dimensional curvature (curvature magnitude and bending direction).
- 2004	2D and 3D shape sensor	Shape sensing was enabled thanks to the development of approaches for shape reconstruction of optical fiber cables with embedded FBGs, by integrating the curvature sensed along the sensor and aligning successive arc segments of fixed curvature.
- 2007	Shape sensor using OFDR	Optical Frequency Domain Reflectometry (OFDR) technique permitted distributed shape sensing based on Rayleigh scattering using an optical multicore fiber.
- 2012	Novel method for 3D shape sensing	An innovative method, based on the numerical resolution of a set of Frenet-Serret equations, was proposed to reconstruct complex three-dimensional fiber shapes as a continuous parametric solution, instead of sequence of arcs.
- 2014	Twisted seven-core multicore fiber	Optical twisted multicore fibers for sensing applications were designed and manufactured to enable twisting compensation in shape sensing, since the use of twisted MCF increases the sensitivity to twisting.
- 2014	Continuous gratings in multicore fiber	An inscription apparatus and a fabrication scheme that allow the continuous inscription of gratings over meters in all cores of multicore fiber through UV transparent coating were proposed. Continuous gratings increase signal to noise ratio and shape sensing precision, compared to the bare Rayleigh scattering of the optical fiber without gratings.
- 2016	Shape sensor using Brillouin scattering	Distributed shape sensing based on Brillouin scattering was performed using an optical multicore fiber and a Brillouin optical time-domain analyzer.
- 2016	Force and shape sensor	A force and shape sensors for medical applications was developed using an optical fiber sensor with embedded FBGs.

Figure 2.7: Historical progress in FOSS

### 2.4.1.3 Application of FOSS

This technology is used in civil engineering for geotechnical monitoring, where landslides and slope movements are a significant hazard that can result in many fatalities and significant property loss, and structural health monitoring of civil infrastructures. Following that, industrial and aerospace engineering for aircraft wiping shape measurement, medical applications in robotics, surgical instruments, posture monitoring, and error analysis are compared. [9]

### 2.4.2 Optical Fibre Humidity Sensors (OFHS)

Optical Fibre Humidity Sensors (OFHS) is composed of an optical fibre structure interacting with humidity-sensitive material. The optical fibre structure includes optical absorption, gratings, interferometers, modal interferometers, resonators and lossy mode resonance.

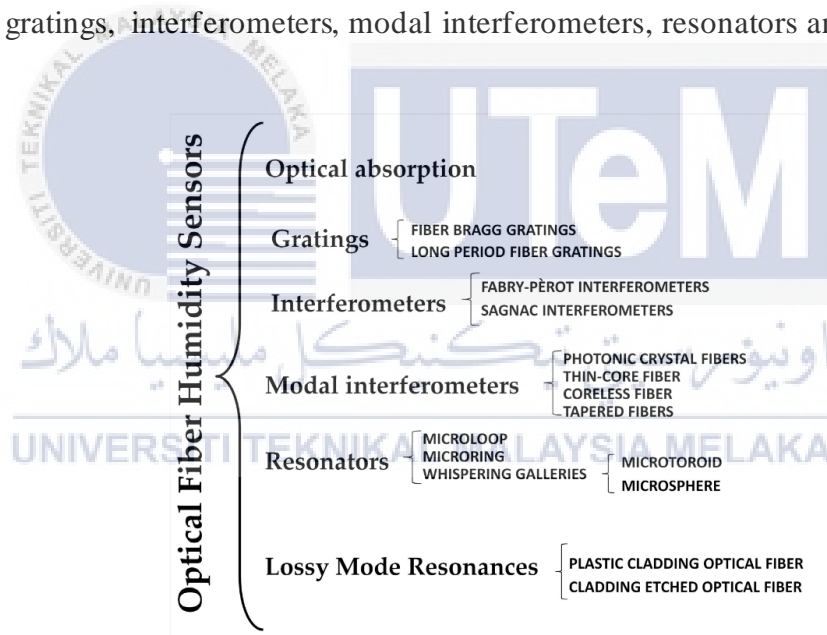


Figure 2.8: Classification of optical fibre humidity sensors

### 2.4.2.1 Optical Absorption Sensors

The interaction of the evanescent field and the coating that serves as the sensitive material causes these sensors to change the transmitted optical power across the entire spectrum. Plastic-cladding silica (PCS) optical fibre or plastic optical fibres (POF) are commonly used for this type of sensor, though other options, such as side-polished optical fibre (D-shape), are available. Although some of these optical fibres have advantages such as low fabrication costs, the ability to measure with a simple setup, and high reliability, they also have disadvantages. The main disadvantages stem from the measurement technique, which only detects changes in optical power transmitted; these changes could be influenced by unfavourable factors such as variations in the light source.

Recent research has concentrated on the investigation of materials that are becoming increasingly common in the development of optical fibre sensors. These materials are being researched to see if they can improve OFHS sensitivity or response time. Zinc oxide, reduced graphene oxide (rGO), and tungsten disulfide have all been investigated.

### 2.4.2.2 Modal Interferometers

The interferometric phase difference is calculated by comparing the effective refractive indices of different fibre modes. Photonic Crystal Fibres (PCF), which are characterised by a complex pattern of microscopic air-holes in the transverse plane that runs all along the fibre, and tapered optical fibres, the most well-known structure being non-adiabatic tapered optical fibres (NATOF), are two types of fibres in a hybrid structure. Following that, modal interferometers were created by splicing a standard SMF to a thin-core optical fibre. Photonic crystal fibres, thin-core fibre, coreless fibre, and tapered fibre are the types of fibres used.

### **2.4.2.3 Resonators and Whispering Galleries Modes**

The optical devices used are microloop and microknot resonators, as well as the whispering galleries mode. The structure of the microloop and microknot resonator exhibits a desired characteristic for all optical sensors, which is a high Q factor. The Q factor is related to the quality of filter performance and implies a higher sensor resolution. There are numerous methods for creating resonators. The waveguide and the coupler are two optical structures that make up the whispering galleries modes resonator. The electromagnetic surface oscillations are supported by the circular structures of the dielectric resonator and are evanescently coupled to the waveguide.

### **2.4.2.4 Optical Fibre Humidity Sensors Based on Lossy Mode Resonances**

Surface plasmon resonances (SPRs) and lossy mode resonances (LMRs) are electromagnetic resonances that produce an attenuation band in the transmitted spectrum. SPRs, on the other hand, transfer energy from light to free electrons of a noble metal, whereas LMRs couple light with a coating. Because they can be observed in both transverse magnetic (TM) and transverse electric (TE) modes, LMRs are more adaptable for use in sensor applications. LMRs have the advantage of producing multiple attenuation bands at tuneable wavelengths. Light resonantly couples to modes guided in the coating, resulting in LMRs. LMR devices are made up of a waveguide coated with a thin film.

For LMR generation, a variety of materials, including metal oxides and polymers, have been tested. Different optical fibre types, including single-mode fibres (SMFs) and plastic-clad silica (PCS) fibres, have been used to develop LMR-based sensors. Performance of LMR is improved by side-polished fibres and cladding etched SMFs. Further enhancing sensor sensitivity can be achieved by combining LMRs with localised surface plasmon resonance (LSPR) or other optical phenomena. [10]

### 2.4.3 Fibre Bragg Grating (FBG)

FBG is an optical structure composed of a periodic perturbation of a waveguide's refractive index. The core of an optical fibre is exposed to an intense optical interference pattern of ultraviolet light to form an FBG. The grating has no effect on light propagating at wavelengths other than the Bragg wavelength, as defined by the equation:  $B=2n$ , where  $B$  is the Bragg wavelength,  $n$  is the grating's effective refractive index in the fibre core, and  $\Lambda$  is the grating period. [10]

#### 2.4.3.1 FBG Sensor Grating Profiles

The use of phase masking allows for the imprinting of various grating profiles, which has a significant impact on the light signal transmitted across the grated OF. Because light wavelength modulation is largely determined by the grating arrangement within the core of an OF, various grating profiles have been considered and studied for their sensing performance. In uniform grating, the period of each grating is distributed uniformly along the sensitised region of an OF, which is a widely used and established grating arrangement. Uniform periodicity gratings are frequently combined with various coatings for environmental sensing.

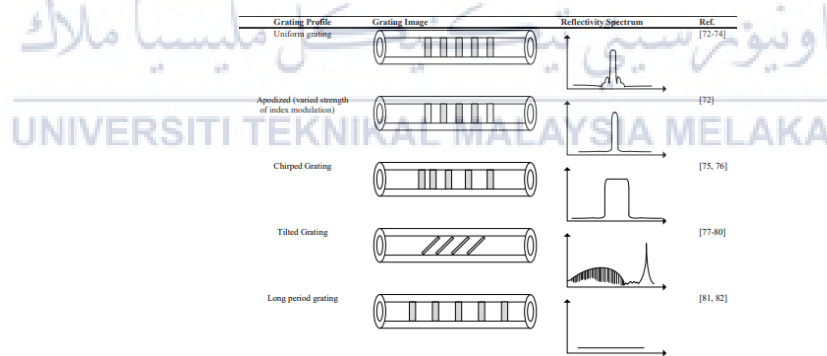


Figure 2.9: Various grating profiles of FBG

### 2.4.3.2 Etching of FBG

A common enhancement made to FBG is by stripping its cladding, reducing its diameter and revealing the core, thus increasing their sensitivity. Avoiding methods, such as flame tapering, that might disturb or reduce the core size is essential to maintaining the integrity of the grating. The cladding is instead stripped without harming the core using D-shaped or side polishing techniques and chemicals like hydrofluoric acid (HF).

The impact of etching the cladding on how the FBG interacts with its surroundings is significant. Changes in the refractive index of the surrounding medium can have an impact on the thinly etched fibre, which is located close to its core. This can cause changes in the wavelength and intensity of the propagated light. Additionally, the etching process can lead to surface irregularities that can result in chirps in the FBG's wavelength spectrum and light propagation scattering.

The performance of the etching is also influenced by where it is located along the FBG fibre. In earlier research, the end of the fibre was typically etched, producing probe-type intrinsic sensors. This positioning results in uniformly etched FBG fibres and reduces the effect of ambient strain during etching. However, this method restricts the ability to multiplex the FBG for multiple point or parameter sensing.

To reduce strain during the etching process, extra care must be taken when etching the middle section of the fibre. The performance of the FBG sensor can be hampered by the chirping that strained fibres can introduce into the Bragg spectrum. This has been countered by using a specially created V-shaped mount to lessen stress on the FBG fibre during etching. The FBG's degree of tension during chemical etching has a big impact on the reflectivity spectrum. The reflectivity peak is maintained while a uniform wavelength shift is guaranteed by optimising fibre tension.

### 2.4.3.3 Coating of FBG

The application of various coatings to Fibre Bragg Grating (FBG) sensors to enable chemical and humidity sensing is covered in the passage. FBGs are sensitised for measuring a variety of parameters using chemical-sensitive coatings. The FBGs can be coated with materials that interact with chemicals in the environment by etching away the cladding.

For sensing humidity, polymer-based materials like polyimides have been used. When these materials are exposed to water molecules, they deform by swelling, putting strain on the fibre core and changing the wavelength that is transmitted. However, polyimides have limitations at higher temperatures.

Coatings made of graphene oxide (GO) have been used to increase moisture sensitivity. The ability of GO to interact with chemical compounds due to its high surface-to-volume ratio makes it possible to detect chemicals and humidity. For humidity sensing, GO-coated FBGs demonstrated an incredibly quick response time.

For FBG sensors, coatings made of organo-silica materials, such as di-ureasil, have been used. Di-ureasil works well as a coating for humidity detection because of its durability and ability to adhere to optical fibres. However, the creation of di-ureasil requires a difficult process that involves urea linkages derived from sol-gels.

FBGs coated with polyaniline have been used to measure pH. Conducting polymer polyaniline demonstrated excellent results with extremely quick response times and high sensitivity to pH. The coating thickness had an impact on the sensor's sensitivity and hysteresis error.

For temperature sensing, ceramic coatings like strontium titanate ( $\text{SrTiO}_3$ ) have been used on FBGs. The  $\text{SrTiO}_3$  smooth film coating shielded the FBG and demonstrated good temperature sensitivity. The pulsed laser deposition method used for coating, though, might not be economical.

For detecting humidity, metallic coatings like zinc oxide have been suggested. High surface-to-volume ratio zinc oxide enables water molecule attachment. The hydrothermal processes used in the coating process led to an increase in humidity sensitivity. [1 1]

## 2.4.4 Polymer Optical Fibre Sensor (POFs)

Polymer Optical Fibres (POFs) have gained popularity in industry and automotive networks due to their reliability, cost-effectiveness, and ease of installation. They are utilised for domestic networks that facilitate the automation and fusion of sensor systems and applications. With benefits like flexibility and lower costs compared to glass fibres, POF sensors are also expanding. Numerous methods utilising optical fibres have been developed in the field of liquid level sensing, including non-intrusive sensors and fibres with the cladding removed. Self-referencing intensity-based sensors that can operate remotely and are unaffected by their surroundings are still in high demand. This paper presents an innovative intensity-based POF sensor for liquid detection. The sensor functions as a coupler, adjusting its coupling ratio based on the refractive index of the surrounding liquid, making it suitable for measuring liquid levels in challenging environments such as oil/petrol tanks or biomass boilers in buildings. Through theoretical analysis and experimental findings, the study demonstrates the capabilities of POF sensors in home networks.

### 2.4.4.1 Principle of Operation and Simulations

The figure for the sensor is shown below, with P1 serving as the input port and P2 and P4 serving as the direct and coupled output ports, respectively. The device's coupling ratio is defined as  $K = P2/(P2 + P4)$ .  $T$ ,  $R$ , and  $g$  are the Fresnel transmission coefficient, curvature radius applied at the sensing area, and gap between the cores of the two fibres at the coupling area, respectively. The parameter indicates the depth of fibre polishing.

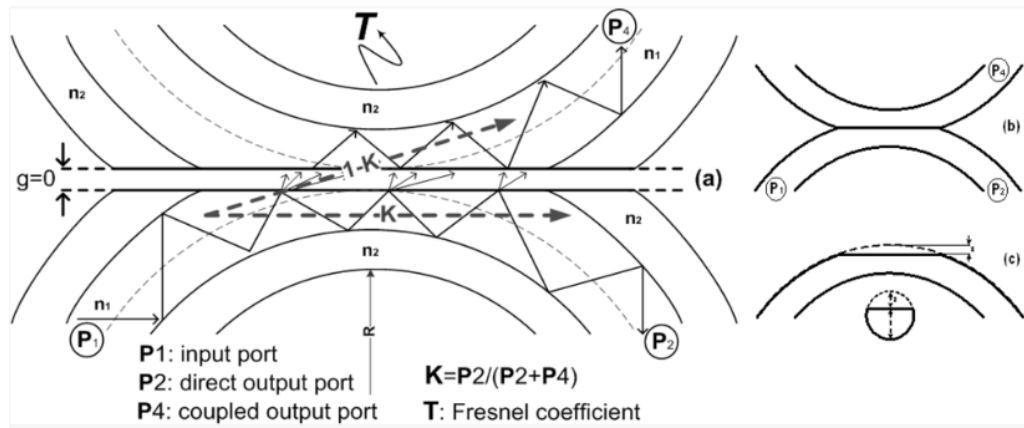


Figure 2.10: (a) Longitudinal section of the coupling (and sensing) area of the POF liquid sensor. (b) POF liquid sensor. (c) One arm sensor fibre after polishing

#### 2.4.4.2 Sensor Measurements

Two standard Step-Index PMMA (polymethylmethacrylate) POFs ( $n_{co} = 1.492$  and  $n_{cl} = 1.417$ ) were used to make the sensor device, each with a section where the cladding was removed and the core was polished (polishing depth = 0.23 0.01 mm). Figure 4 depicts the measurement setup procedure. At the reception stage, a laser diode (Roithner, lessons III) operating at  $\lambda = 630 \text{ nm}$  was used to illuminate the POF fibre, and a two-input power metre was chosen. The POF sensor was sandwiched between two POF fibres and immersed in a tank filled with water first, then with oil as the external liquids.

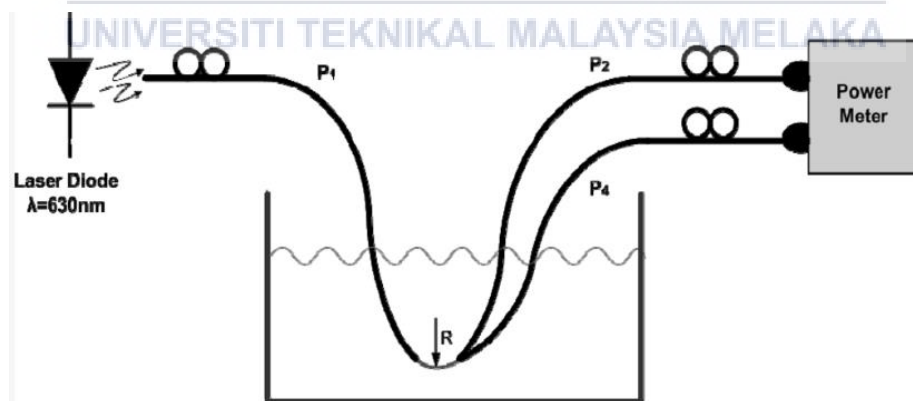


Figure 2.11: POF sensor set-up to determine liquid level in tanks [12]

## 2.5 Advantages and Disadvantages of Fibre Optics

As we know, the two most common types of optical fibre cable used in communication networks are single mode fibre and multimode fibre. The differences in type are determined by the cable's specification and purpose. Even though optical fibre cable has outperformed coaxial cable, the technology is still far from perfect. They still face financial and technological limitations. Engineers can now assess the benefits of optical fibre communication over metallic-based communication systems thanks to technological advancements. The following is a list of optical fibre cable's advantages and disadvantages.

### Advantages:

1. Can be used for access systems with long ranges up to 100km.
2. Supports highspeed and bandwidth up to 10Gbps for about 10km.
3. Single-mode fibre cable costs less than half the price of multimode cable.
4. The only option for fibre network distribution due to its high long-distance performance.
5. Extremely high bandwidth.
6. Easy to accommodate with increasing bandwidth.
7. Resistance to electromagnetic interference.
8. Early detection of cable damage and secure transmissions.
9. Easy to install and is compatible with digital technology.
10. Lightness and small size of the cable, capable of carrying large number of signals.

### Disadvantages:

1. Single mode connectors and pigtail cables are very expensive due to the small core diameter.
2. The manufacture of single mode fibre requires more time and effort due to the small core diameter.
3. Single mode requires more expensive laser diodes than LEDs.
4. Single mode fibre conversion equipment, accessories and devices are very expensive.
5. High installation costs.
6. Susceptibility to physical damage during installation or construction activities.
7. Wildlife damage to fibre optic cables.

8. Requires special training skills.
9. Can be affected by chemicals such as hydrogen gas.

Joining of the fibre optic cables must be good or it will cause lots of attenuation.

[13][14]

## 2.6 Journal Comparison from Previous Work Related to the Project

Table 2.1: Journal Comparison

No	Title	Author	Source	Finding
1	Fibre Optic Microarrays	[1]	Finding optic microarrays	Measurements of fibre optic
2	Structural health monitoring of concrete structures using fibre-optic-based sensors: A review	[2]	Fibre Optic Sensors	Fibre Optic Sensors
3	Fibre Optic Methods of Prospecting: A Comprehensive and Modern Branch of Geophysics	[3]	Basic structure of Optical Fibre	Basic structure of Optical Fibre
4	Single Mode Fiber Standards: A review	[4]	Single-mode fibre types	Dispersion of types of single-mode fibre
5	Fibre Optic Communications: An Overview	[5]	Classification of fibres	SMF, MMF
6	Optical Fibre Communication – An Overview	[6]	Classification of fibres	Multimode Step-Index Fibre

7	Tapered optical fibre sensor for detection of hydrocarbon spills in seawater	[7]	Propagation of light among fibre	Propagation of light among fibre
8	Numerical Aperture of A Plastic Optical Fiber	[8]	Numerical Aperture (NA)	NA, Snell's Law
9	Fiber Optic Shape Sensors: A comprehensive review	[9]	Fibre Optic Shape Sensor	FOSS, strain sensing technology, application
10	Recent Developments in Fiber Optics Humidity Sensors	[10]	Fibre Optics Humidity Sensors	Classifications and types
11	FBG Sensors for Environmental and Biochemical Applications - A Review	[11]	FBG sensors	FBG grating profile, etching, coating
12	A Self-Referencing Intensity Based Polymer Optical Fiber Sensor for Liquid Detection	[12]	Polymer Optical Fibre Sensors	Principle, sensor measurements
13	Indepth Study of Single mode Optical Fibre	[13]	Single mode optical fibre	Advantages & disadvantages
14	Merits And Demerits of Optical Fiber Communication	[14]	Optical fibre communication	Advantages & disadvantages

## 2.7 Summary

In this chapter, various analyses and techniques for optical loop fibre humidity sensors were covered. The studies found out different methods were used to create the fibre optic sensors. There are various types and materials of fibre optic sensors with different ways to experiment humidity. Fibre-optic sensing technology is a promising alternative to traditional moisture/humidity monitoring since it has various advantages over traditional sensing methods. As a result, the review concludes with a thorough analysis of the various types of optical fibre sensing technologies used in the study to measure humidity. Lastly, it is a good idea to review many approaches that have been published over the years with most of them focusing on sensory qualities acquired in a controlled laboratory setting.



## CHAPTER 3

### METHODOLOGY

#### 3.1 Introduction

The methodology of this project is a set of principles that describes the project's flow from the beginning to ending. The methods used in this chapter and the rest of the experiment are stripping, cleaving, splicing and looping of the optical fibre. The following are the list of tools required to complete the process.

##### 1. Single Mode Fibre Pigtaills

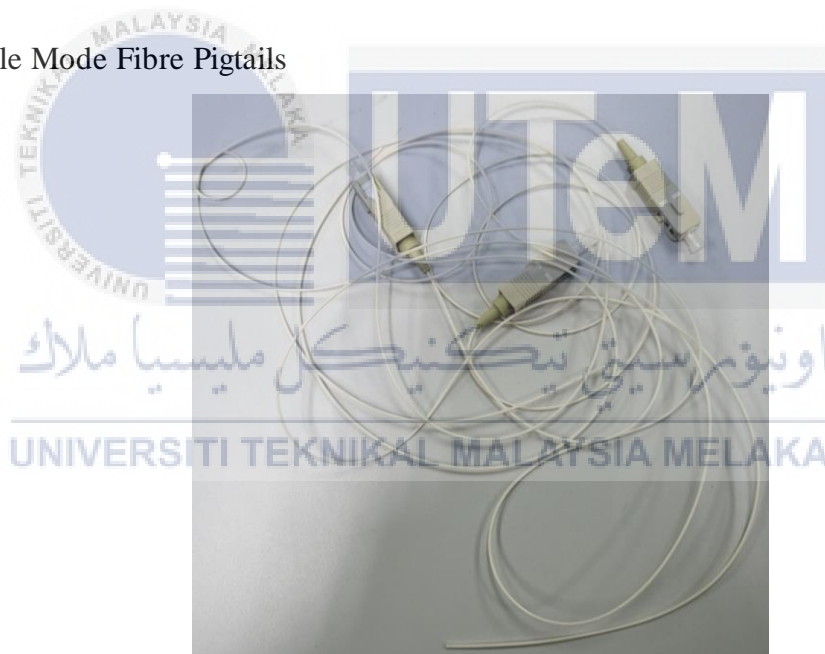


Figure 3.1: A pair of SC/UPC connectors for Single Mode Fibre Pigtaills

## 2. Fibre Optic Cable Cutter



Figure 3.2: The Cutter to cut fibre optic cables

## 3. Fibre Optic Stripper



Figure 3.3: The stripper to remove the outer jacket or coating of fibre optic cables

#### 4. Isopropyl Alcohol



Figure 3.4: Cleaning tool used after stripping fibre optic cables

#### 5. Hand Cleaver



Figure 3.5: Fujikura Hand Cleaver used to cut the fibre tips to the proper length for splicing

## 6. Fusion Splicer



Figure 3.6: Fusion splicer machine which splits two fibres together automatically

## 7. Calcium Chloride



Figure 3.7: Calcium Chloride used for this experiment.

8. Amplified Spontaneous Emitter (ASE)



Figure 3.8: Light source that transmits wavelength of 1310nm and 1550nm light.

9. Mini Pro Optical Time Domain Reflectometer (OTDR)



Figure 3.9: Pulsed laser light flowing via an optical fibre is transmitted and analysed during OTDR testing.

### 3.2 Project Flow

Once supervision is found, the project title was given. After understanding and researching about the project, the problem statements and objectives were determined. Then the literature review was done to examine and identify the needs used in this project.

The experiment sets were developed after doing the literature review. The experiment is conducted with a 100% until 50% dehumidifier. Two SMF28 optical cables were required, a laser source with wavelengths of 1310nm and 1550nm and a Mini Pro Optical Time Domain Reflectometer (OTDR). After preparing the apparatus, the data will be recorded for 5 minutes, starting with humidity level of 100%. Then, the final data will be recorded. Lastly, the optical microfibre double loop sensor for humidity will be built after this research.

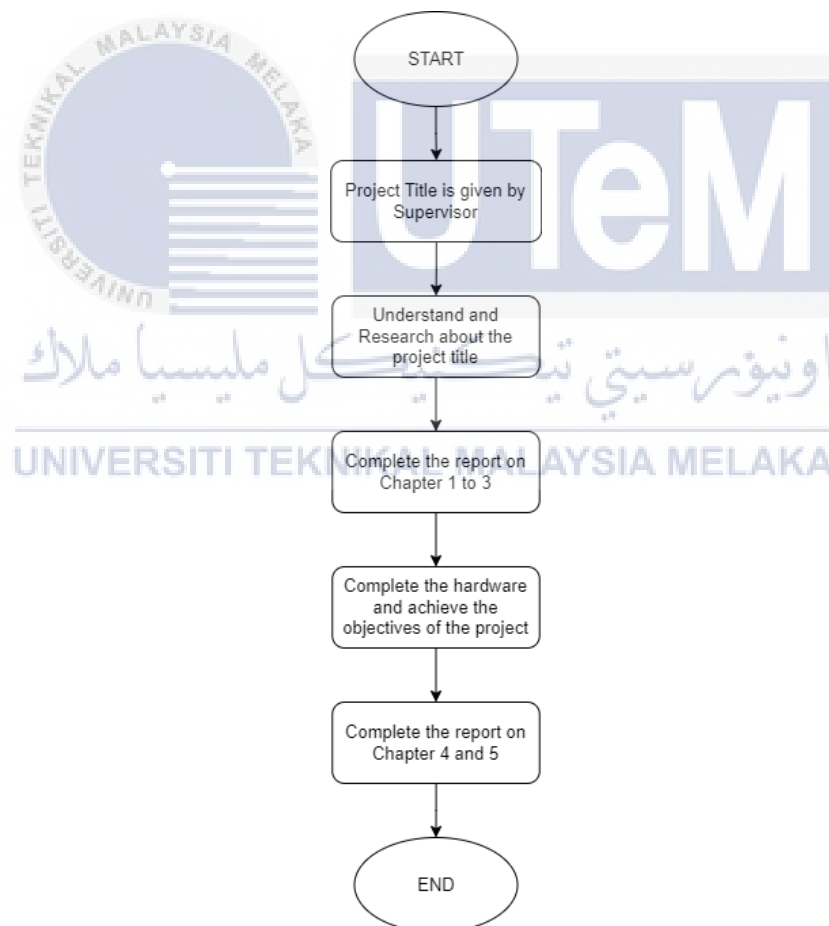


Figure 3.10: The project flow of this report

### 3.3 Procedure

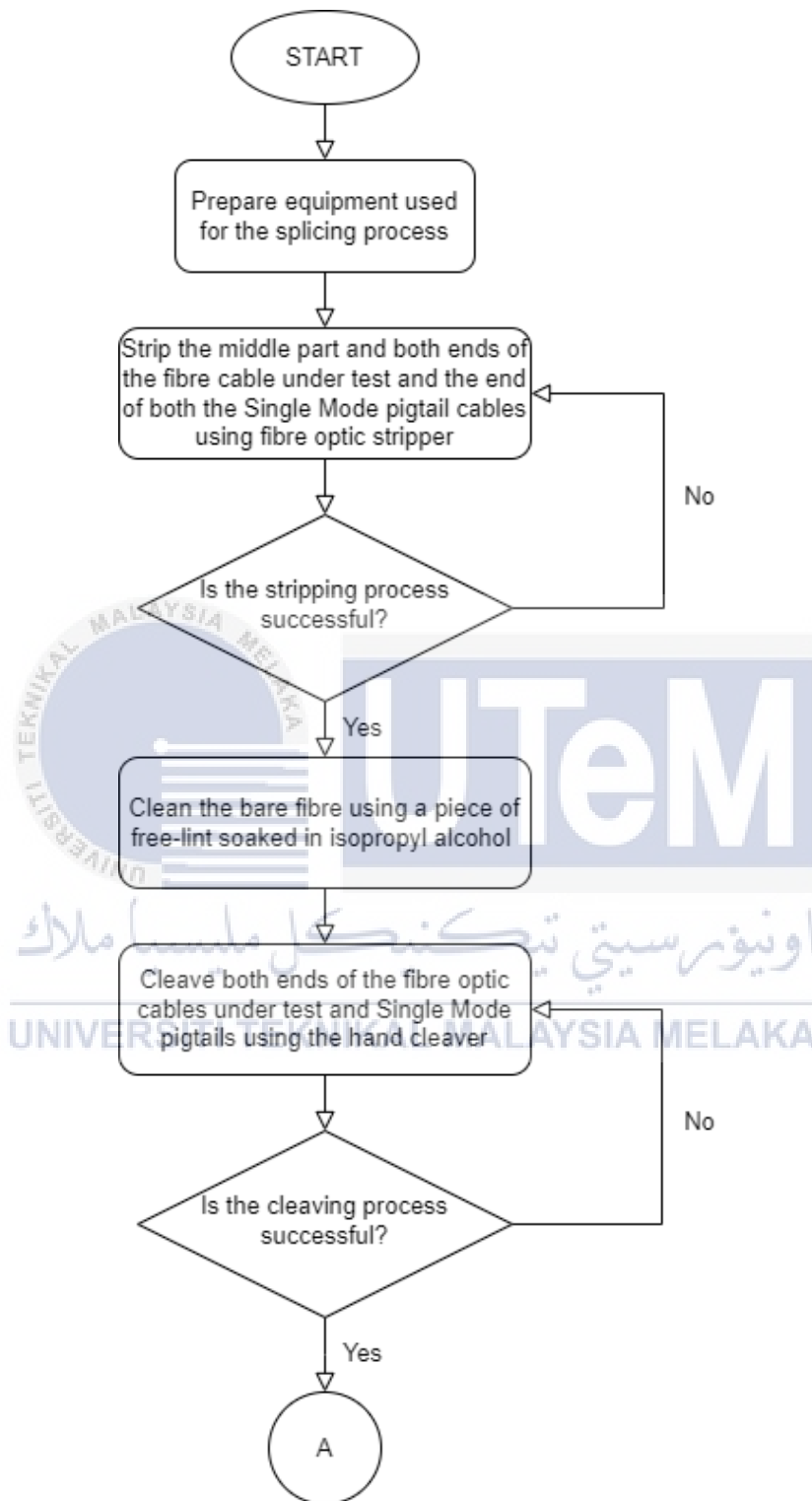


Figure 3.11: The flowchart of stripping, cleaning and cleaving the fibre optic cable.

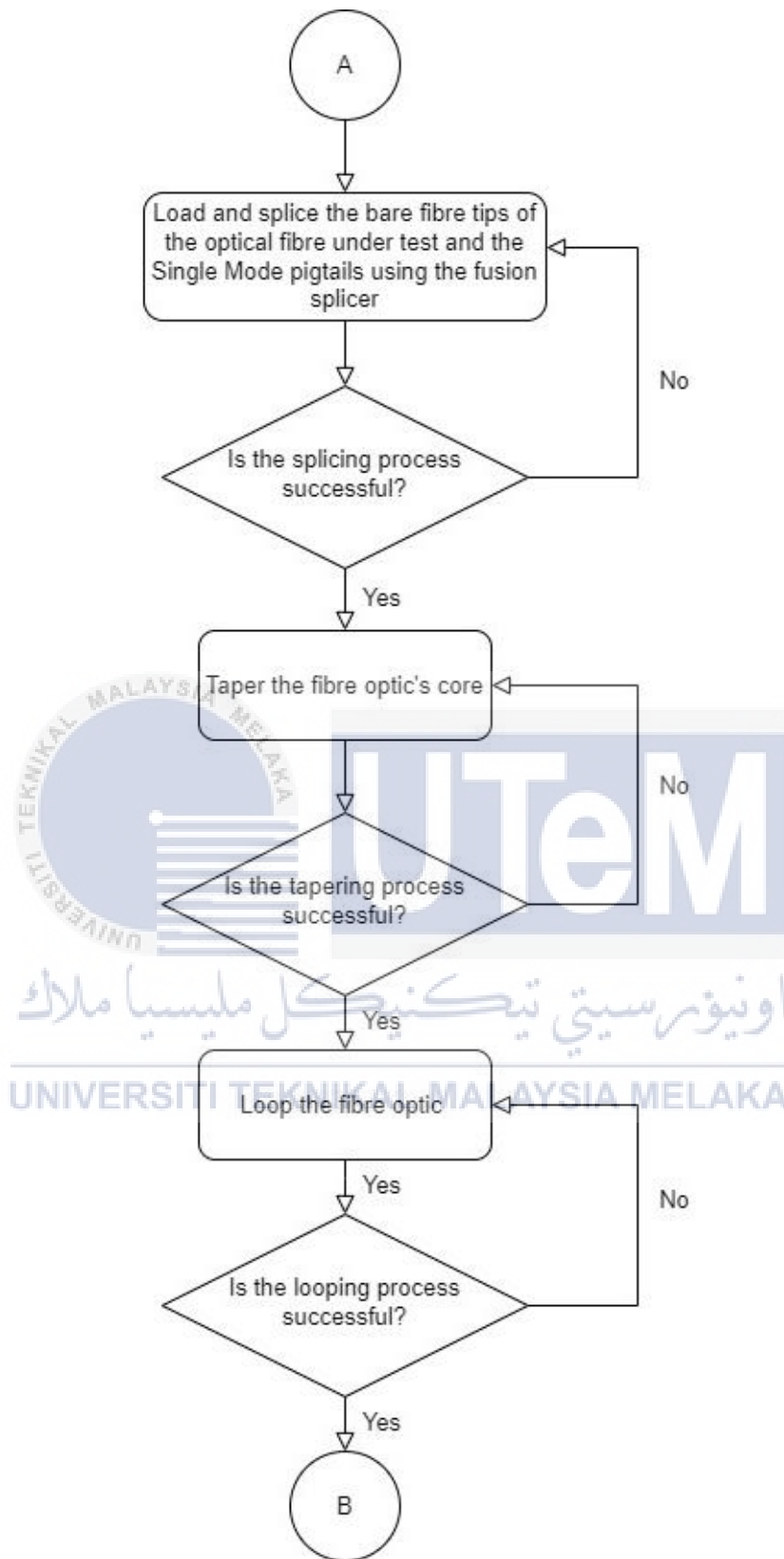


Figure 3.12: The flowchart of splicing, tapering and looping the fibre optic cable.

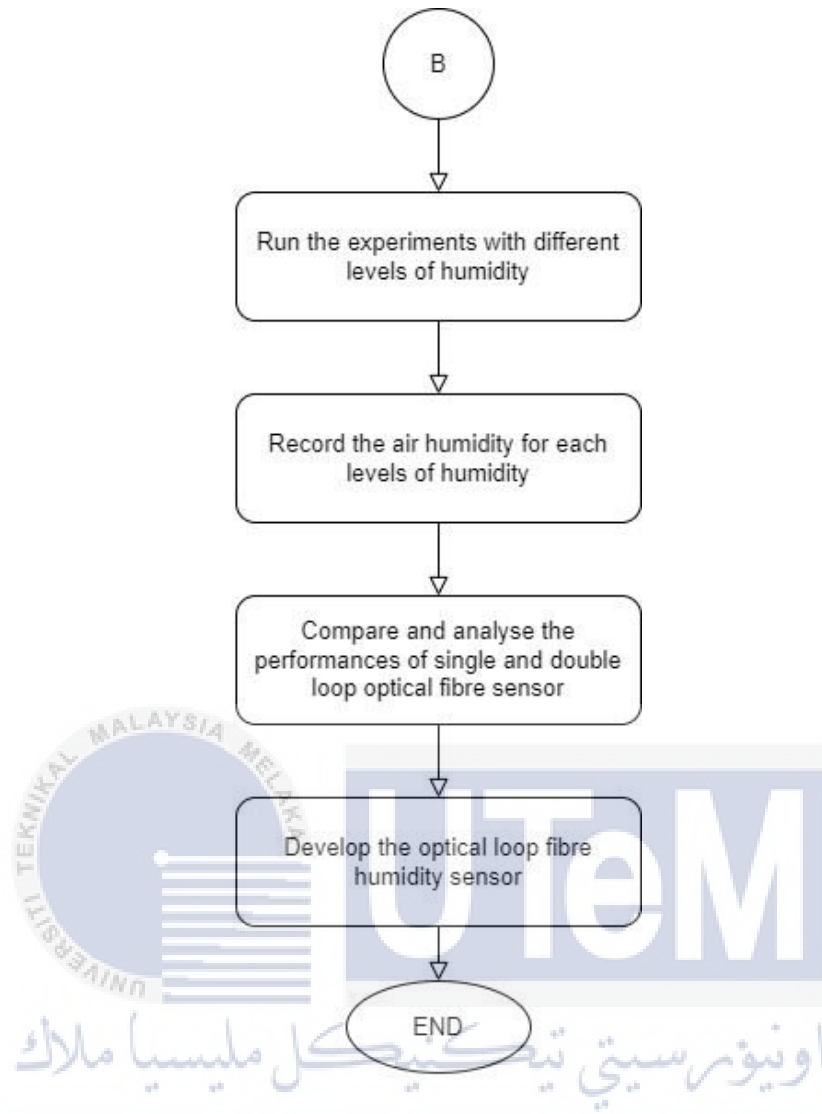


Figure 3.13: The flowchart of conducting the experiment in developing fibre optic as a sensor.



### 3.3.2 Stripping Process

The stripper tool is used to cut the outer jacket or coating of the fibre optic cable in preparation for fusion splicing. The holes in the stripper blade are normally laser cut to precise tolerance. The opening is large enough for the stripper to cut without breaking the fibre glass.



Figure 3.15: The process of stripping the fibre optic cable.

UNIVERSITI TEKNIKAL MALAYSIA MELAKA

### 3.3.3 Cleaning Process

Once the plastic cladding has been removed from the fibre optic cables, the bare fibre will be cleaned using a piece of free-lint tissue soaked in isopropyl alcohol until it makes a squeaky sound. This action keeps impurities from lingering inside a spliced fibre optic line which will cause splice loss.



Figure 3.16: The process of cleaning the stripped fibre optic cable.

### 3.3.4 Cleaving Process

The fibre's tip surface might not be a pristine, flat surface during the fibre cutting process. Before two fibre optic cables are spliced together, a cleaver must be used to make a clean break on the ends. This is to guarantee that the cables are connected smoothly.



Figure 3.17: The process of cleaving the fibre optic cable.

UNIVERSITI TEKNIKAL MALAYSIA MELAKA

### 3.3.5 Splicing Process

Splicing is the technique of utilizing a splicing machine to join two stripped fibre optic cables. A fibre optic fusion splicer is a machine that uses an electric arc to fuse two fibres. To avoid improper splicing, the total loss, including splice loss along the cable must be shallow to achieve the highest transmission rate.



Figure 3.18: The process of splicing the fibre optic cable.

UNIVERSITI TEKNIKAL MALAYSIA MELAKA

### 3.3.6 Tapering Process

The process is made and carried out to produce a microfibre sensor loop. In this process, the fibre's core will be burned using an equipment created by Dr. Ashadi. This process requires a lot of patience because there is a risk of affecting the microfibre such as being broken.



Figure 3.19: The process of tapering the fibre optic cable.

### 3.3.7 Looping Process

This process is used to increase interaction length and enhance the signal strength of the fibre optic cable. By looping, it allows for higher degree of signal modulation which results in more accurate and precise measurements.

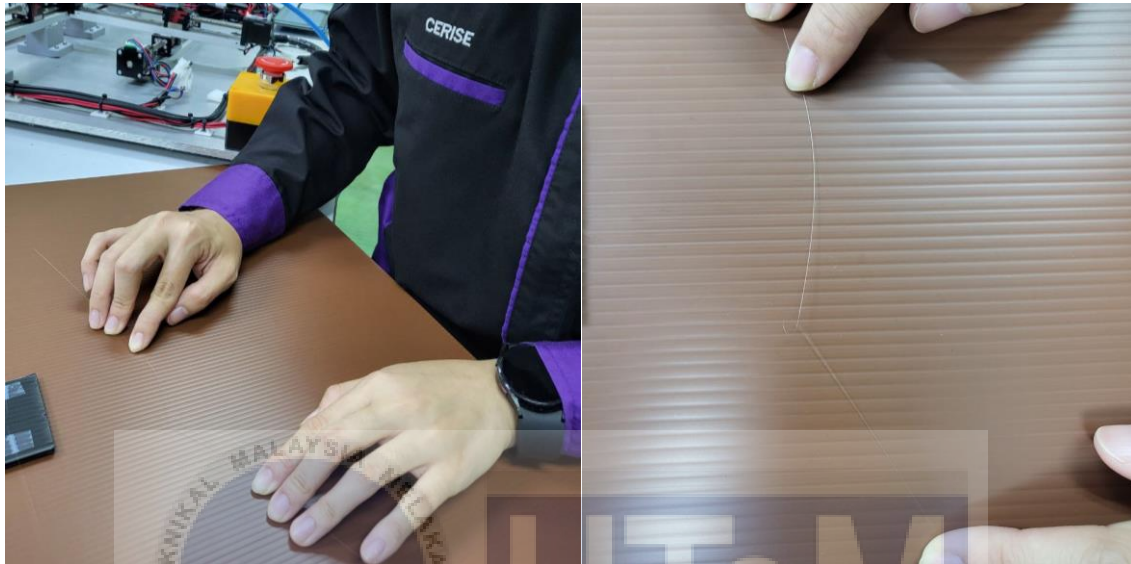


Figure 3.20: The process of looping the fibre optic cable.

اونيورسيتي تيكنيكل مليسيا ملاك  
UNIVERSITI TEKNIKAL MALAYSIA MELAKA

### 3.3.8 Final Check on Fibre

This technique is carried out to ensure the fibre is in good shape. This process is suggested due to concerns over the fibre's condition if it breaks or the laser light does not reach its end. This circumstance is possible because somewhere might go wrong during the tapering process where the fibre core is burnt and transformed into microfibre. The most dangerous is looping part where the fibre will break because it is very fragile and thin. The laser test procedure is done to check the condition of the fibre optic connection.

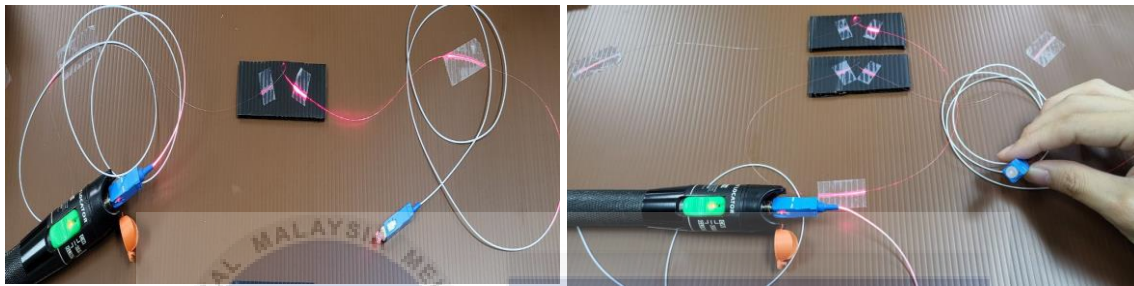


Figure 3.21: The process of testing fibre connection using laser.



### 3.3.9 Measuring of Fibre

This process is to measure the humidity of single and double loop resonators. Starting from 0 calcium carbonate to 5 calcium carbonate in 7 minutes. The graphs and analysis will be done after this process.



Figure 3.22: The process of measuring humidity.



Figure 3.23: The process of measuring humidity of single loop (left) and double loop (right) resonator.

### 3.4 Characterization of Fibre Optic Loop Sensor

When conducting this experiment, known as the characterization of the fibre optic loop sensor, multiple evaluations of the experimental setup are performed to access the capabilities. To ensure that the fibre can carry traffic and serve as a reference for further debugging and troubleshooting, fibre characterization examines insertion loss, optical return loss, polarisation and dispersion.

#### 3.4.1 Connector Inspection

Airborne dirt particles are about the size of the core of an SM fibre and are typically silica-based; if not removed, they may scratch PC connectors. To prevent connectors from being contamination by touching or damaged from dropping, it is recommended to always keep the dust cap of connectors on. Before every testing procedure, it is recommended to clean the connectors first by using lint-free pads and 99% isopropyl alcohol to wet clean the connectors then dry it using dry lint-free pads.



Figure 3.24: Cleaning kit for connectors.

### 3.4.2 Insertion Loss Test

The insertion loss test attempts to replicate the working conditions of the line by powering the optical fibre or cable under test with the test source and measuring the attenuation at the other end with the power meter. The power meter and test source are installed between the fibre optic cable and this experiment's test source. Before connecting with the optical fibre, the power meter is set to 0dB when the source is turned on.

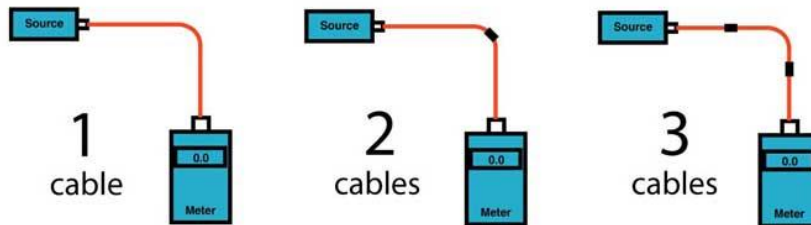


Figure 3.25: 0dB reference at power meter then to test the insertion loss.

### 3.4.3 Reflectance and Return Loss Test

Reflectance is the optical return loss for individual events. For an example, the reflection above the fibre backscatter level relative to the source pulse. For passive optics, optical return loss is measured in decibels (dB) and is always negative, with values closer to 0 representing larger reflections (poorer connections). Optical Return Loss (ORL) is the return loss for the entire fibre under test, including fibre backscatter and reflections, relative to the source pulse. It is also expressed in decibels (dB), but it is always positive, with values closer to 0 dB representing more total light reflected.

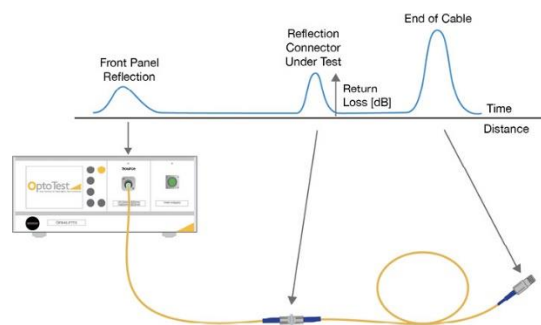


Figure 3.26: Return loss testing.

### 3.4.4 Polarization Mode Dispersion

Polarisation mode dispersion (PMD) is a type of modal dispersion in which two different polarisations of light in a waveguide travel at different speeds due to random imperfections and asymmetries, resulting in random spreading of optical pulses. There are three types of dispersion in fibre optics which are modal dispersion (MMF), chromatic dispersion where and polarization mode dispersion where each component reaches the receiver at a slightly different time to broaden the received pulse.

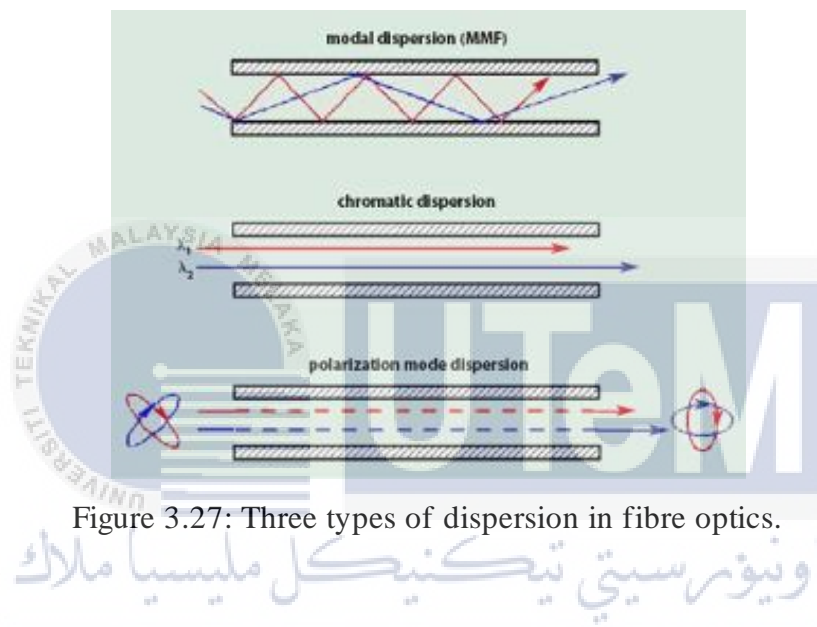


Figure 3.27: Three types of dispersion in fibre optics.

### 3.5 Summary

Overall, the first flowchart is guidance on how the report is done. The second flowchart is about the procedure of stripping, cleaning, cleaving, splicing, tapering, looping and experimenting with the final product. Lastly is the four characterization of fibre loop which are connector inspection, insertion loss test, reflectance and return loss test and polarization mode dispersion. This chapter also covers the whole process of microfibre double looping process until the testing phase.

## CHAPTER 4

### RESULTS AND DISCUSSIONS

#### 4.1 Introduction

This chapter explained the results and data analysis on the development of an optical microfiber humidity loop sensor for the medical industry. A variety of tests are used to determine how well the project is performed. The sensor's performance will be evaluated using these criteria, which include its sensitivity and linearity, test results, operational capabilities, and repeatability. It is critical to note that the purpose of these tests is to aid in the development of the sensor.

#### 4.2 Size of Microfiber Optical Loop Sensor

Figure 4.1 shows the new size of the microfiber optic sensor. The size of microfiber sensor has been measured using a microscope. The microfiber sensor was successfully produced by combustion during tapering process. The size of the fibre has been reduced from  $125\mu\text{m}$  to  $15\mu\text{m}$ .

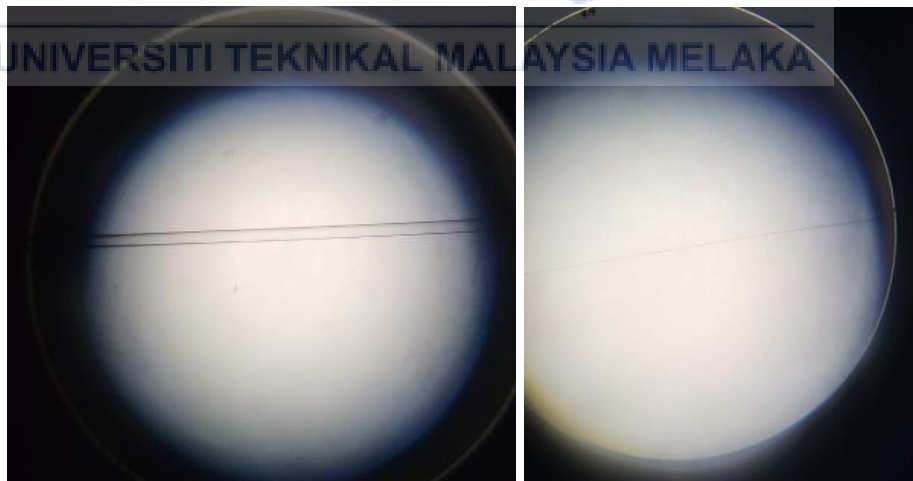


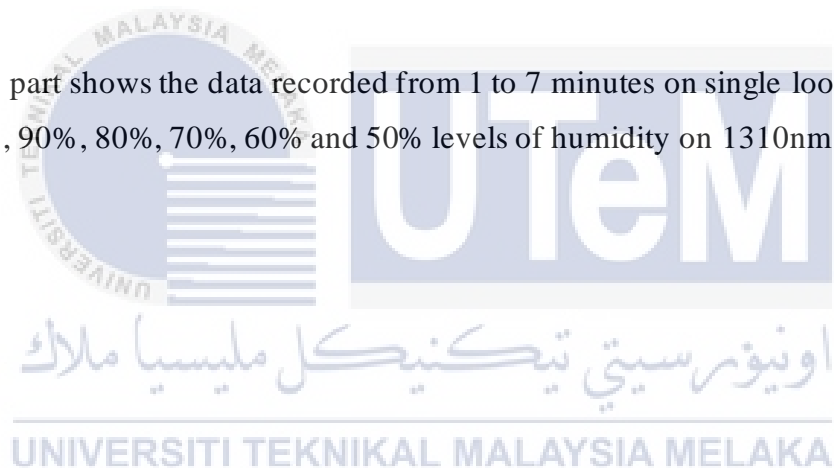
Figure 4.1: New Size of the Microfiber optic sensor (right).

### 4.3 Result and Analysis for Humidity over Time using Calcium Chloride

The experiment involves sending a modulated light source to an optical time domain reflectometer (OTDR) via two single-mode fibre pigtails joined at the splice with a length of an unclad region in the transmission's centre and loop. The transmission from the light source will be uneven because some light particles have been evaporated from the core of the optical cable. This study includes two different wavelengths which are 1310nm and 1550nm and two types of looping which are single loop and double loop. This study is also taken in increments of 1 minute to 7 minutes. The results will vary depending on the humidity percentage used. This section contains data collected at various intervals of one minute to seven minutes for single and double loop resonator.

#### 4.3.1 Single Loop Resonator

This part shows the data recorded from 1 to 7 minutes on single loop resonator by using 100%, 90%, 80%, 70%, 60% and 50% levels of humidity on 1310nm and 1550nm.



#### 4.3.1.1 100% of Humidity (0 pieces of Calcium Chloride) Tested on 1310nm and 1550nm Wavelengths

Table 4.1: Recorded Data for 100% Humidity

Time (mins)	Output Power (-dBm)	
	1310nm	1550nm
1	40.86	38.34
2	42.38	39.40
3	43.47	40.01
4	44.09	40.04
5	44.42	40.11
6	44.61	40.16
7	44.86	40.19

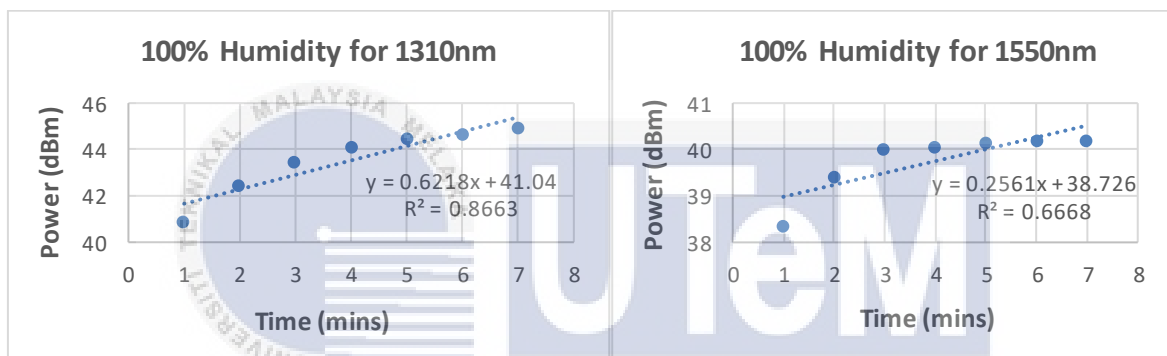


Figure 4.2: Microfiber Optic Single Loop Sensor at 100% Humidity.

Based on the table and the two graphs above, the data shows that power increases linearly with time. For 1310nm, the sensitivity is 0.6218 whereas for 1550nm, the sensitivity is 0.2561. By comparing both graphs, it is concluded that for 100% humidity, 1310nm is more sensitive than 1550nm.

### 4.3.1.2 90% of Humidity (1 piece of Calcium Chloride) Tested on 1310nm and 1550nm Wavelengths

Table 4.2: Recorded Data for 90% Humidity

Time (mins)	Output Power (-dBm)	
	1310nm	1550nm
1	41.00	39.94
2	43.80	40.49
3	44.19	40.62
4	44.22	40.68
5	44.30	40.72
6	44.34	40.73
7	44.35	40.74

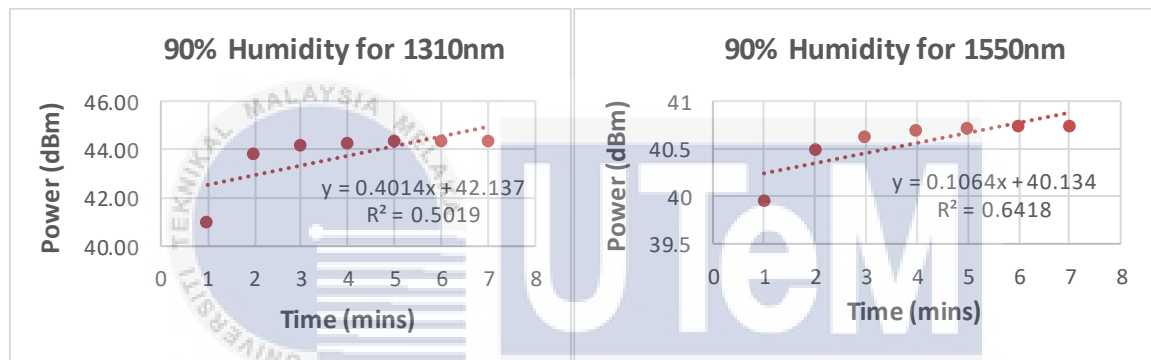


Figure 4.3: Microfiber Optic Single Loop Sensor at 90% Humidity.

According to the data in the table and the two graphs above, power increases linearly with time. The sensitivity for 1310nm is 0.4014, while the sensitivity for 1550nm is 0.106. By comparing the two graphs, it is determined that 1310nm is more sensitive than 1550nm at 90% humidity.

### 4.3.1.3 80% of Humidity (2 pieces of Calcium Chloride) Tested on 1310nm and 1550nm Wavelengths

Table 4.3: Recorded Data for 80% Humidity

Time (mins)	Output Power (-dBm)	
	1310nm	1550nm
1	42.05	38.13
2	44.16	39.21
3	44.90	39.89
4	45.08	40.44
5	45.12	40.57
6	45.20	40.62
7	45.22	40.66

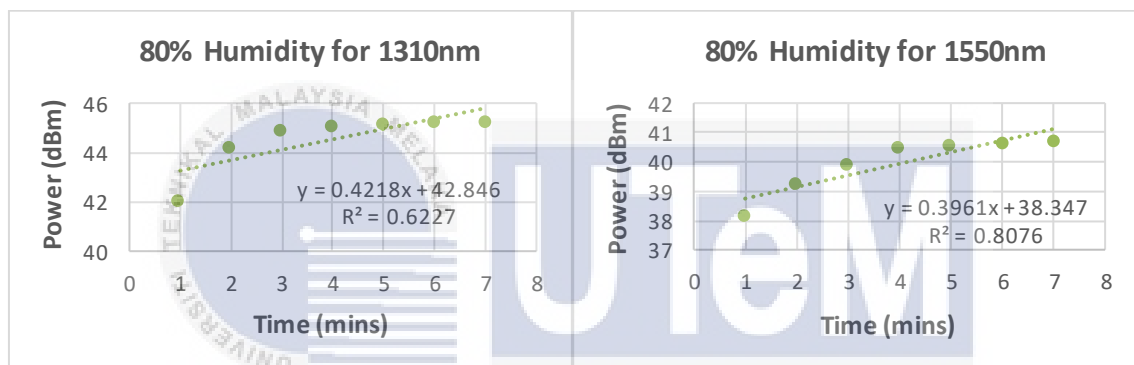


Figure 4.4: Microfiber Optic Single-Loop Sensor at 80% Humidity.

Based on the table and the two graphs above, the data shows that power increases linearly with time. For 1310nm, the sensitivity is 0.4218 whereas for 1550nm, the sensitivity is 0.3961. By comparing both graphs, it is concluded that for 80% humidity, 1310nm is more sensitive than 1550nm.

#### 4.3.1.4 70% of Humidity (3 pieces of Calcium Chloride) Tested on 1310nm and 1550nm Wavelengths

Table 4.4: Recorded Data for 70% Humidity

Time (mins)	Output Power (-dBm)	
	1310nm	1550nm
1	42.78	38.12
2	43.74	39.38
3	43.87	39.69
4	44.02	39.86
5	44.10	39.93
6	44.11	39.95
7	44.13	39.96

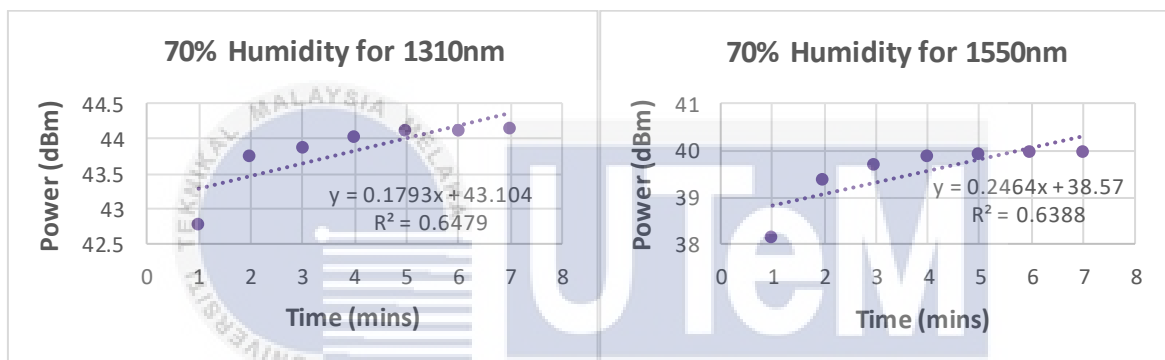


Figure 4.5: Microfiber Optic Single Loop Sensor at 70% Humidity.

According to the data in the table and the two graphs above, power increases linearly with time. The sensitivity for 1310nm is 0.1793, while the sensitivity for 1550nm is 0.2464. By comparing the two graphs, it is determined that 1550nm is more sensitive than 1310nm at 70% humidity.

### 4.3.1.5 60% of Humidity (4 pieces of Calcium Chloride) Tested on 1310nm and 1550nm Wavelengths

Table 4.5: Recorded Data for 60% Humidity

Time (mins)	Output Power (-dBm)	
	1310nm	1550nm
1	42.88	40.33
2	43.28	40.45
3	43.35	40.79
4	43.38	41.39
5	43.41	41.80
6	43.43	42.13
7	43.40	42.15

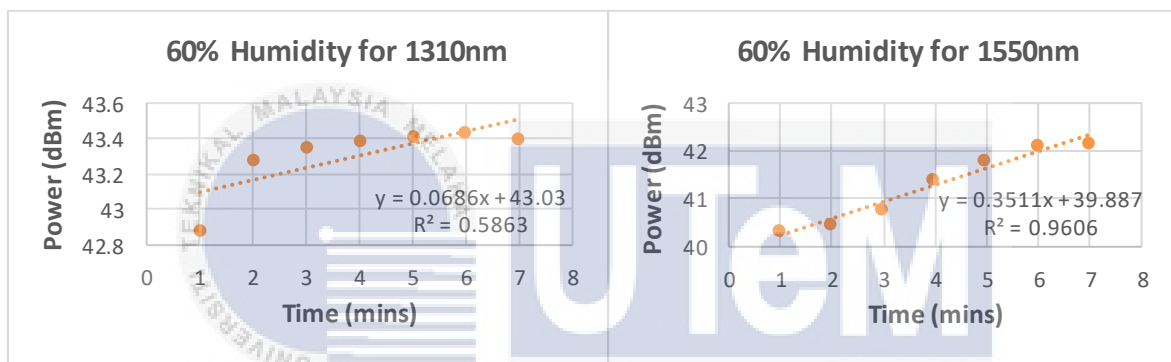


Figure 4.6: Microfiber Optic Single Loop Sensor at 60% Humidity.

Based on the table and the two graphs above, the data shows that power increases linearly with time. For 1310nm, the sensitivity is 0.0686 whereas for 1550nm, the sensitivity is 0.3511. By comparing both graphs, it is concluded that for 60% humidity, 1550nm is more sensitive than 1310nm.

### 4.3.1.6 50% of Humidity (5 pieces of Calcium Chloride) Tested on 1310nm and 1550nm Wavelengths

Table 4.6: Recorded Data for 50% Humidity

Time (mins)	Output Power (-dBm)	
	1310nm	1550nm
1	41.36	39.48
2	42.89	39.57
3	44.51	39.95
4	44.83	40.02
5	45.06	40.03
6	45.14	40.05
7	45.24	40.08

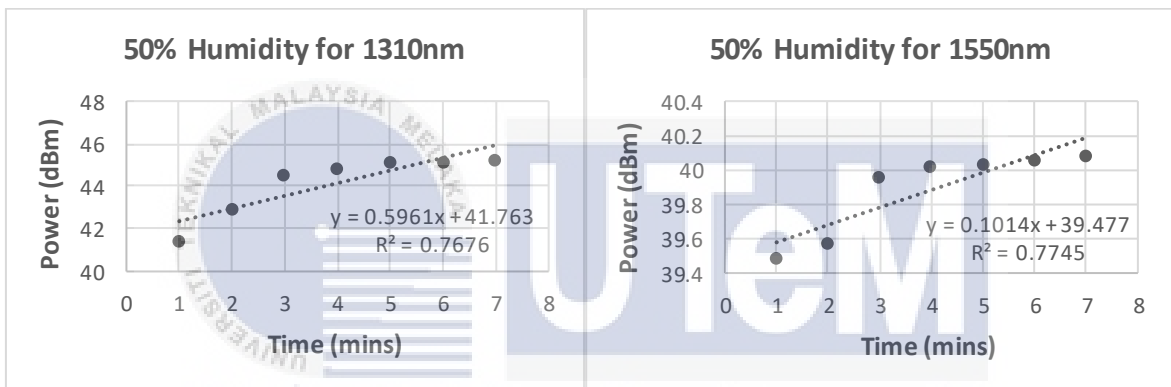


Figure 4.7: Microfiber Optic Single Loop Sensor at 50% Humidity.

According to the data in the table and the two graphs above, power increases linearly with time. The sensitivity for 1310nm is 0.5961, while the sensitivity for 1550nm is 0.1014. By comparing the two graphs, it is determined that 1310nm is more sensitive than 1550nm at 50% humidity.

#### 4.3.1.7 Comparison

Table 4.7: Recorded Data for Comparison of Humidity (%) and 1310nm and 1550nm Wavelengths for Single Loop Resonator

Humidity (%)	1310nm		1550nm	
	Sensitivity (dBm)	Linearity (%)	Sensitivity (dBm)	Linearity (%)
100	0.6218	93.08	0.2561	81.66
90	0.4014	70.84	0.1064	80.11
80	0.4218	78.91	0.3961	89.87
70	0.1793	80.49	0.2464	79.92
60	0.0686	76.57	0.3511	98.01
50	0.5961	87.61	0.1014	88.01

From the table above, it can be concluded that 100% humidity has the highest sensitivity of 0.6218dBm for 1310nm whereas 80% humidity has the highest sensitivity of 0.3961dBm for 1550nm. Among the data for the whole table, the best sensitivity for single loop resonator is 100% for 1310nm.

### 4.3.2 Double Loop Resonator

This part shows the data recorded from 1 to 7 minutes on double loop resonator by using 100%, 90%, 80%, 70%, 60% and 50% levels of humidity on 1310nm and 1550nm.

#### 4.3.2.1 100% of Humidity (0 pieces of Calcium Chloride) Tested on 1310nm and 1550nm Wavelengths

Table 4.8: Recorded Data for 100% Humidity

Time (mins)	Output Power (-dBm)	
	1310nm	1550nm
1	52.38	47.99
2	53.45	49.20
3	53.47	50.00
4	53.77	50.02
5	53.79	50.11
6	53.82	50.13
7	53.85	50.24

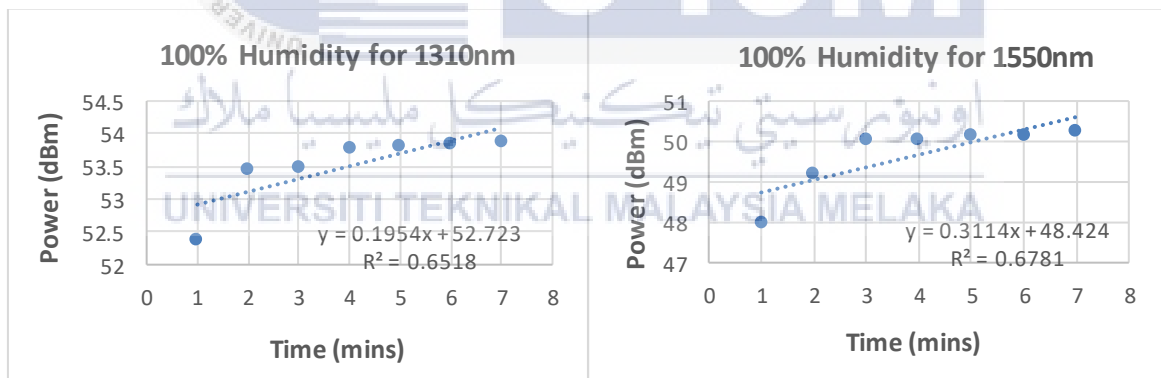


Figure 4.8: Microfiber Optic Single Loop Sensor at 100% Humidity.

According to the data in the table and the two graphs above, power increases linearly with time. The sensitivity for 1310nm is 0.1954, while the sensitivity for 1550nm is 0.3114. By comparing the two graphs, it is determined that 1550nm is more sensitive than 1310nm at 100% humidity.

### 4.3.2.2 90% of Humidity (1 piece of Calcium Chloride) Tested on 1310nm and 1550nm Wavelengths

Table 4.9: Recorded Data for 90% Humidity

Time (mins)	Output Power (-dBm)	
	1310nm	1550nm
1	48.03	48.47
2	48.73	49.11
3	48.72	49.38
4	49.12	49.56
5	49.27	49.60
6	49.43	49.76
7	49.47	49.85

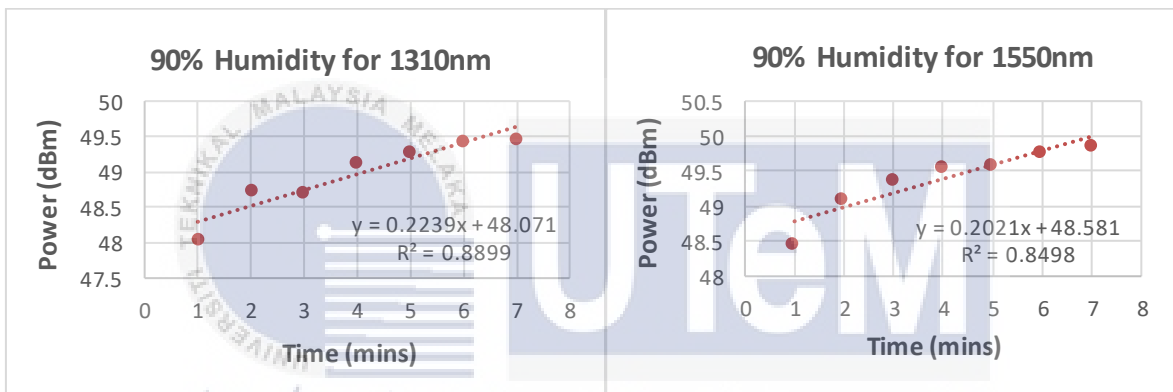


Figure 4.9: Microfiber Optic Single Loop Sensor at 90% Humidity

Based on the table and the two graphs above, the data shows that power increases linearly with time. For 1310nm, the sensitivity is 0.2239 whereas for 1550nm, the sensitivity is 0.2021. By comparing both graphs, it is concluded that for 90% humidity, 1310nm is more sensitive than 1550nm.

### 4.3.2.3 80% of Humidity (2 pieces of Calcium Chloride) Tested on 1310nm and 1550nm Wavelengths

Table 4.10: Recorded Data for 80% Humidity

Time (mins)	Output Power (-dBm)	
	1310nm	1550nm
1	52.52	50.51
2	52.71	50.60
3	53.87	51.04
4	55.01	51.07
5	55.45	51.36
6	55.64	51.46
7	55.83	51.50

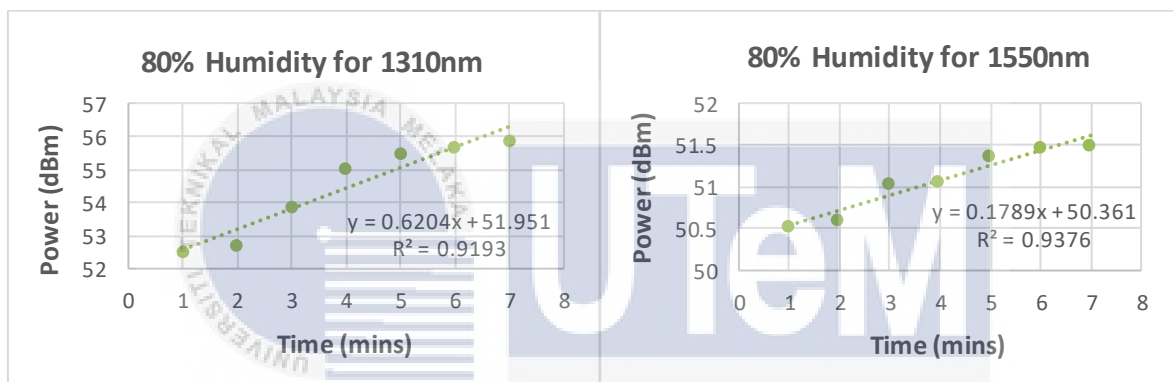


Figure 4.10: Microfiber Optic Single Loop Sensor at 80% Humidity.

According to the data in the table and the two graphs above, power increases linearly with time. The sensitivity for 1310nm is 0.6204, while the sensitivity for 1550nm is 0.1789. By comparing the two graphs, it is determined that 1310nm is more sensitive than 1550nm at 80% humidity.

#### 4.3.2.4 70% of Humidity (3 pieces of Calcium Chloride) Tested on 1310nm and 1550nm Wavelengths

Table 4.11: Recorded Data for 70% Humidity

Time (mins)	Output Power (-dBm)	
	1310nm	1550nm
1	49.12	45.52
2	51.35	46.20
3	52.26	46.85
4	52.33	46.99
5	52.49	47.18
6	53.04	47.31
7	53.22	47.98

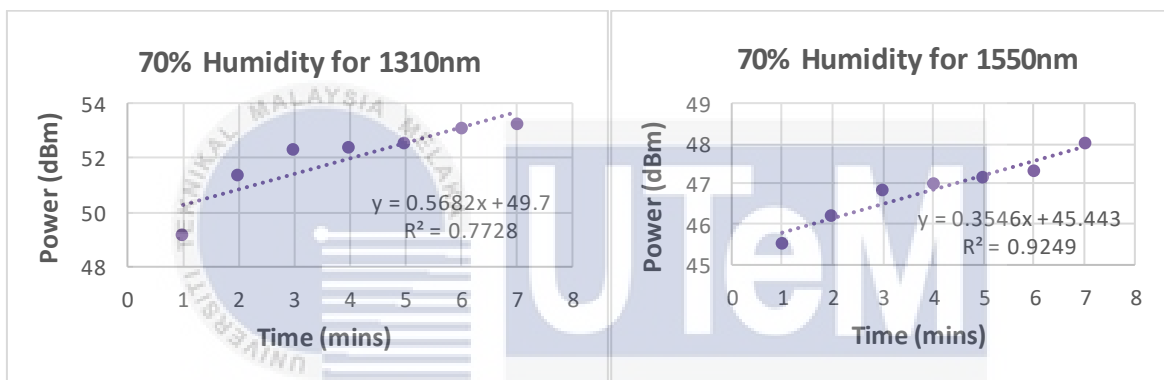


Figure 4.11: Microfiber Optic Single Loop Sensor at 70% Humidity.

Based on the table and the two graphs above, the data shows that power increases linearly with time. For 1310nm, the sensitivity is 0.5682 whereas for 1550nm, the sensitivity is 0.3546. By comparing both graphs, it is concluded that for 70% humidity, 1310nm is more sensitive than 1550nm.

#### 4.3.2.5 60% of Humidity (4 pieces of Calcium Chloride) Tested on 1310nm and 1550nm Wavelengths

Table 4.12: Recorded Data for 60% Humidity

Time (mins)	Output Power (-dBm)	
	1310nm	1550nm
1	43.80	45.75
2	45.79	46.18
3	46.11	46.19
4	46.34	46.53
5	46.36	46.61
6	47.17	46.72
7	47.20	46.76

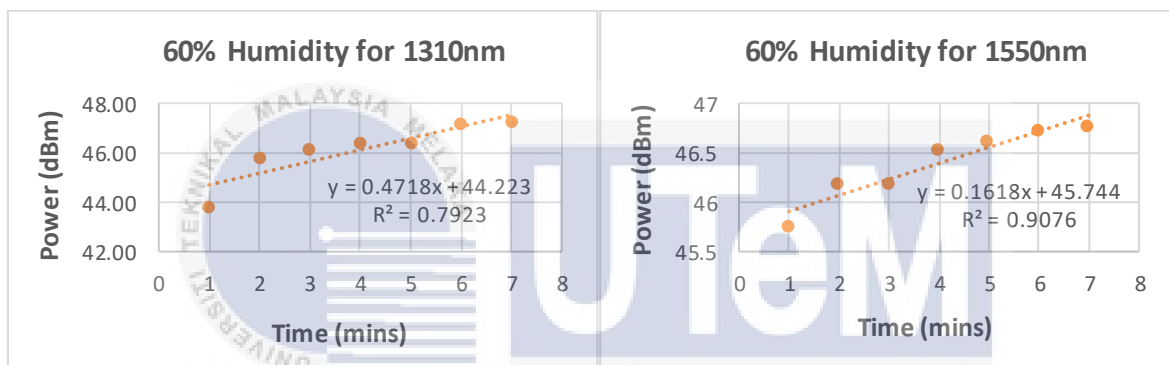


Figure 4.12: Microfiber Optic Single Loop Sensor at 60% Humidity.

According to the data in the table and the two graphs above, power increases linearly with time. The sensitivity for 1310nm is 0.4718, while the sensitivity for 1550nm is 0.1618. By comparing the two graphs, it is determined that 1310nm is more sensitive than 1550nm at 60% humidity.

#### 4.3.2.6 50% of Humidity (5 pieces of Calcium Chloride) Tested on 1310nm and 1550nm Wavelengths

Table 4.13: Recorded Data for 50% Humidity

Time (mins)	Output Power (-dBm)	
	1310nm	1550nm
1	44.59	48.26
2	44.78	49.00
3	44.97	49.31
4	45.01	49.42
5	45.05	49.55
6	45.12	49.61
7	45.15	49.64

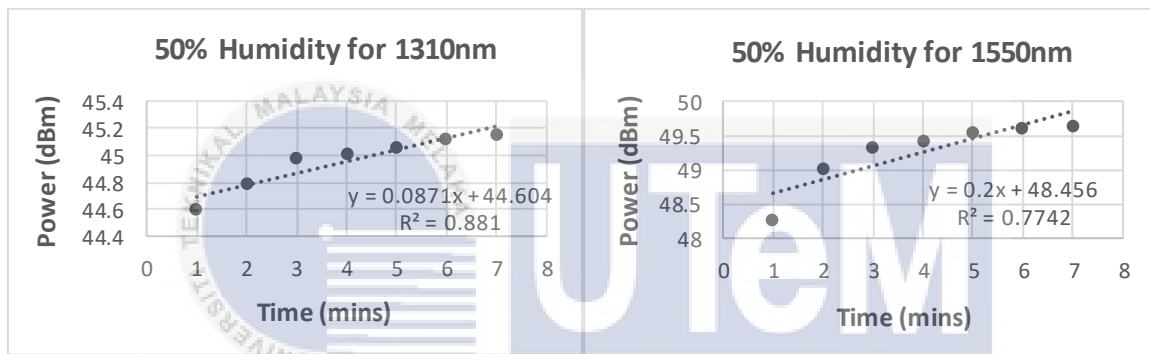


Figure 4.13: Microfiber Optic Single Loop Sensor at 50% Humidity.

Based on the table and the two graphs above, the data shows that power increases linearly with time. For 1310nm, the sensitivity is 0.0871 whereas for 1550nm, the sensitivity is 0.2. By comparing both graphs, it is concluded that for 50% humidity, 1550nm is more sensitive than 1310nm.

#### 4.3.2.7 Comparison

Table 4.14: Recorded Data for Comparison of Humidity (%) and 1310nm and 1550nm Wavelengths for Double Loop Resonator

Humidity (%)	1310nm		1550nm	
	Sensitivity (dBm)	Linearity (%)	Sensitivity (dBm)	Linearity (%)
100	0.1954	80.73	0.3114	82.35
90	0.2239	94.33	0.2021	92.18
80	0.6204	95.88	0.1789	96.83
70	0.5682	87.91	0.3546	96.17
60	0.4718	89.01	0.1618	95.27
50	0.0871	93.86	0.2000	87.99

From the table above, it can be concluded that 80% humidity has the highest sensitivity of 0.6204dBm for 1310nm whereas 70% humidity has the highest sensitivity of 0.3546dBm for 1550nm. Among the data for the whole table, the best sensitivity for double loop resonator is 80% for 1310nm.

#### 4.4 Analysis of Results of the Average of Microfibre Interaction with Power over Humidity

This section shows the comparison of average power of 7 minutes and humidity of single and double loop resonator along with 1310nm and 1550nm wavelengths.

##### 4.4.1 Comparison of Average Power of Single and Double Loop Resonator for Different Levels of Humidity for 1310nm

Table 4.15: Recorded Data for Comparison of Average Power (dBm) and Humidity (%) of Single and Double Loop resonator at 1310nm

Humidity (%)	Average Power (dBm)	
	Single Loop	Double Loop
100	43.527	53.504
90	43.743	48.967
80	44.533	54.433
70	43.821	51.973
60	43.304	46.11
50	44.147	44.953

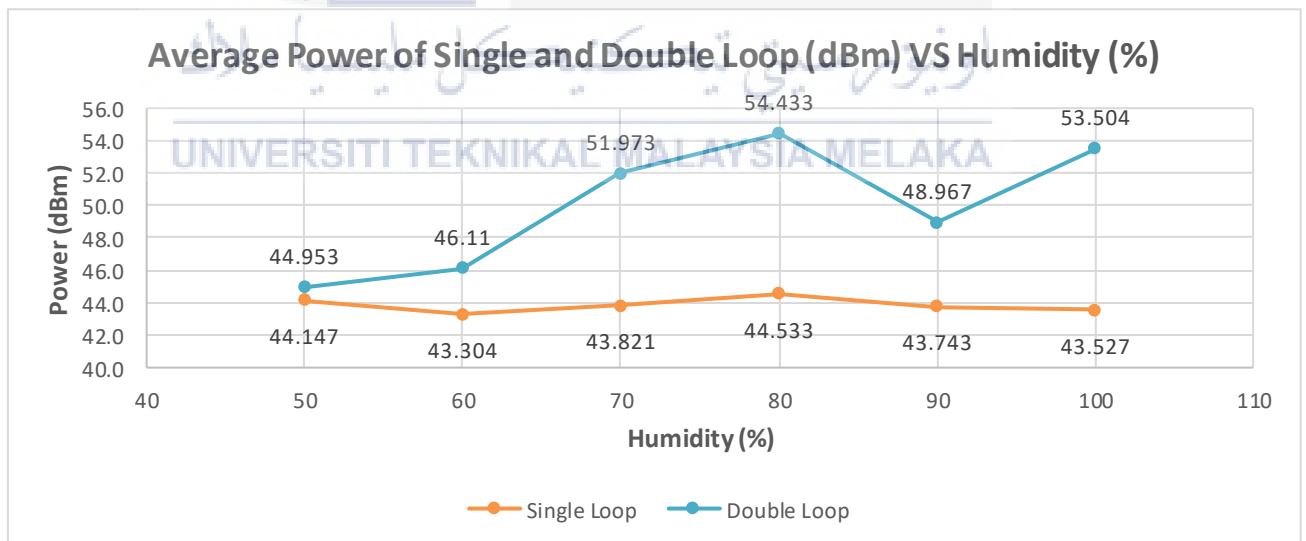


Figure 4.14: Fibre Optic Sensor for Average Power of Single and Double Loop of 1310nm.

From the table and graphs above for 1310nm wavelength, we can see that for each humidity, the average power of single loop resonator is lower than double loop resonator. This shows that the more the loops, the higher the power.

#### 4.4.2 Comparison of Average Power of Single and Double Loop Resonator for Different Levels of humidity for 1550nm

Table 4.16: Recorded Data for Comparison of Average Power (dBm) and Humidity (%) of Single and Double Loop resonator at 1550nm

Humidity (%)	Average Power (dBm)	
	Single Loop	Double Loop
100	39.75	49.67
90	40.56	49.39
80	39.931	51.077
70	39.556	46.861
60	41.291	46.391
50	39.883	49.256

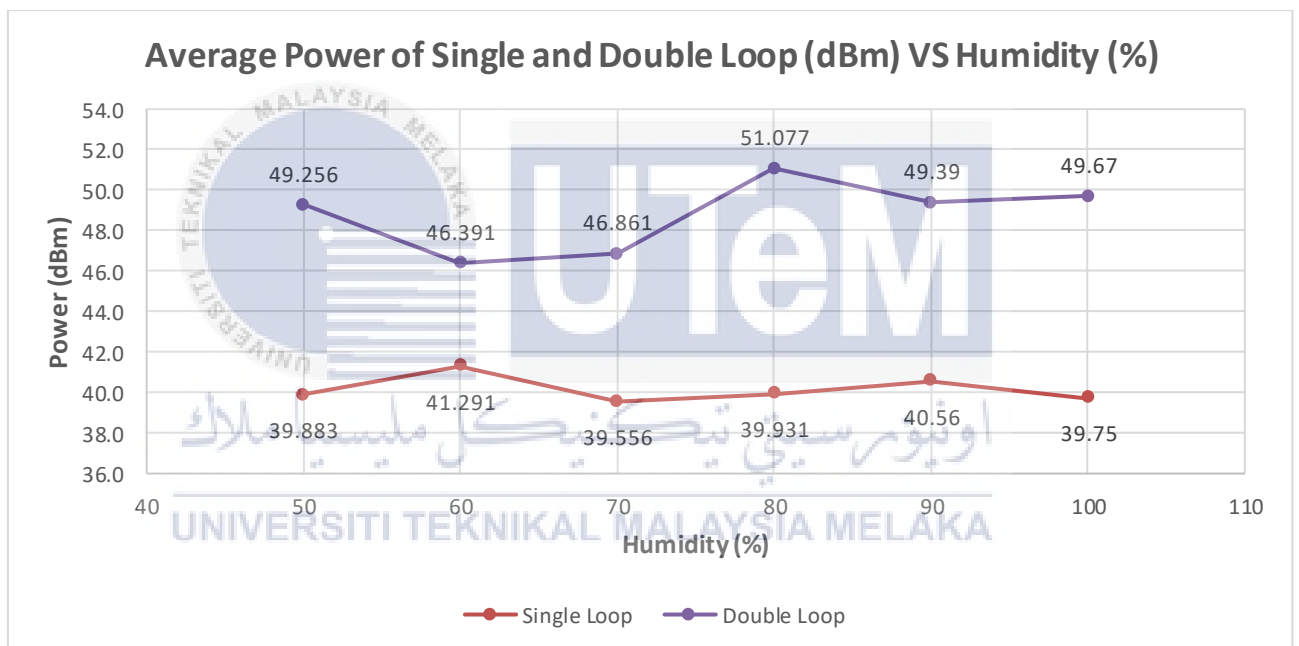


Figure 4.15: Fibre Optic Sensor for Average Power of Single and Double Loop of 1550nm.

From the table and graphs above for 1550nm wavelength, we can also see that for each humidity, the average power of single loop resonator is lower than double loop resonator which is the same as 1310nm. This shows that the more the loops, the higher the power and the wavelength does not affect then power.

#### 4.4.3 Comparison of Average Power of 1310nm and 1550nm Wavelengths for Single Loop at Different Levels of Humidity

Table 4.17: Recorded Data for Comparison of Average Power (dBm) and Humidity (%) of 1310nm and 1550nm

Humidity (%)	Average Power (dBm)	
	1310nm	1550nm
100	43.527	39.75
90	43.743	40.56
80	44.533	39.931
70	43.821	39.556
60	43.304	41.291
50	44.147	39.883

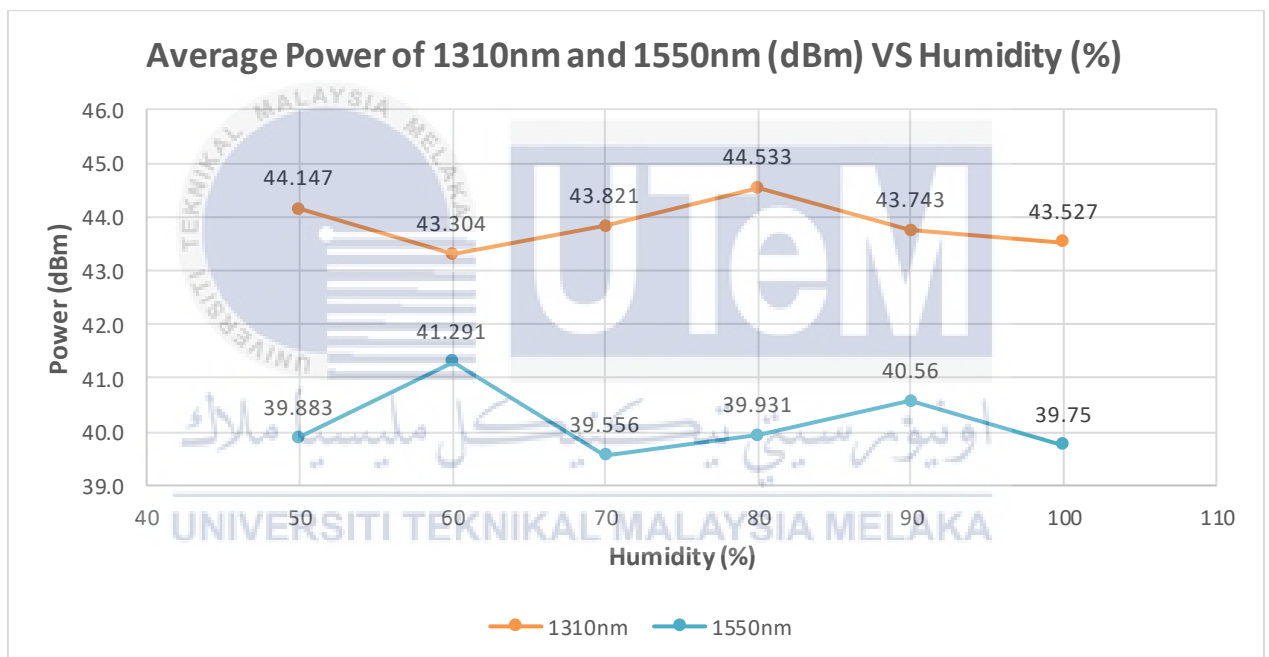


Figure 4.16: Fibre Optic Sensor for Average Power of 1310nm and 1550nm Wavelength for Single Loop.

Based on the table and graph above for single loop resonator, we can see that the average power for 1550nm is lower than 1310nm for each humidity. This shows that the higher the wavelength, the lower the power.

#### 4.4.4 Comparison of Average Power of 1310nm and 1550nm Wavelengths for Double Loop for Different Levels of Humidity

Table 4.18: Recorded Data for Comparison of Average Power (dBm) and Humidity (%) of 1310nm and 1550nm

Humidity (%)	Average Power (dBm)	
	1310nm	1550nm
100	53.504	49.67
90	48.967	49.39
80	54.433	51.077
70	51.973	46.861
60	46.11	46.391
50	44.953	49.256

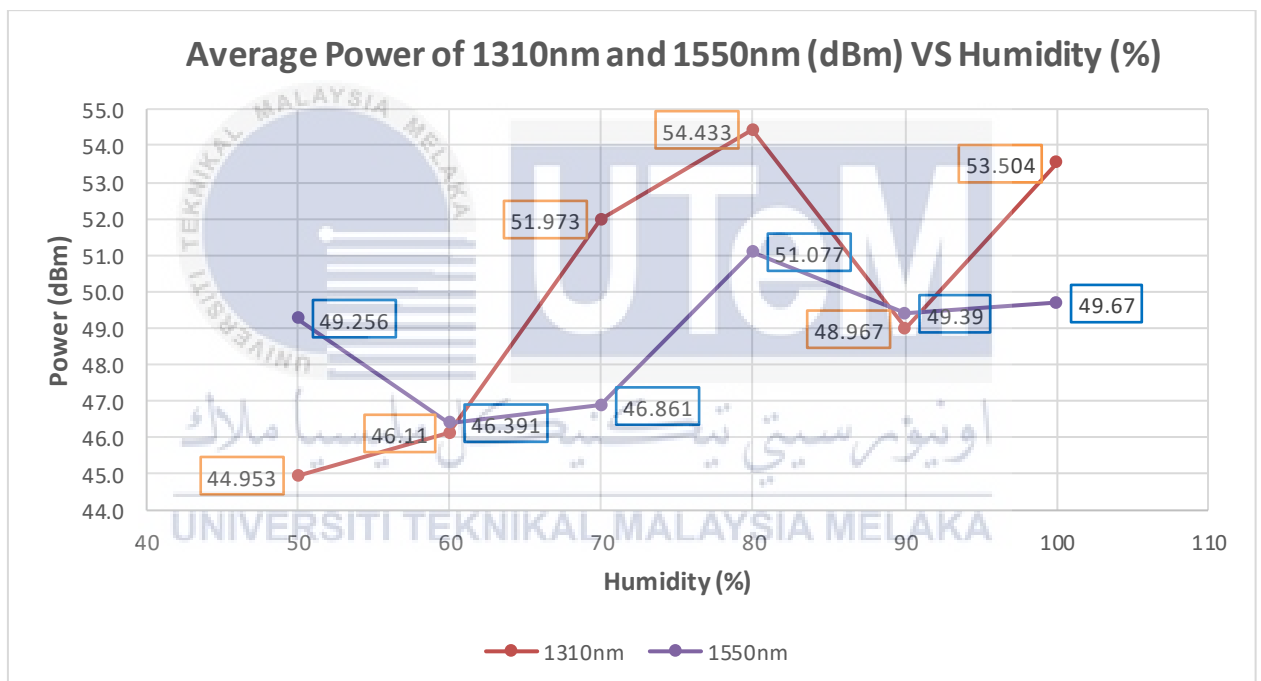


Figure 4.17: Fibre Optic Sensor for Average Power of 1310nm and 1550nm Wavelength of Double Loop.

Based on the table and graph above for double loop resonator, we can see that the average power for 1550nm is lower than 1310nm for 70%, 80% and 100% humidity whereas is slightly higher for 50%, 60% and 90% humidity. On average, the humidity is mostly lower. This also shows that the higher the wavelength, the lower the power.

## CHAPTER 5

### CONCLUSION AND RECOMMENDATIONS

#### 5.1 Conclusion

This chapter summarised the Development of Humidity sensors using Optical Fiber for agricultural industry specifically in greenhouses to adjust the humidity and optimize crop production. This project is conducted based on previous research and literature review from various universities regarding optical fibre as sensor in the agricultural industry. Developing the sensor for the agricultural industry is important as it is needed for plant optimal growth conditions and the prevent plant stress such as waterlogging or dehydration. By doing this, problems can be detected early to save energy and cost. This project's methodology involves stripping, cleaving, splicing, tapering and looping the optical fibre cables. All the methods stated above are implemented to complete the project. This project study is tested with a dehumidifier agent which is Calcium Chloride. It is used to measure the sensitivity of the humidity sensor using optical fibre. Then, the data of comparing the dehumidifier agents in terms of their ability to absorb moisture and water molecule in a confined space are recorded in form of tables. Started from 100% humidity (0 Calcium Carbonate) to 50% humidity (5 Calcium Carbonate) for both single and double loop. The comparisons are then done in graph form for clearer visualization. All measurements are done under the same conditions and environment.

The project's data indicates that relative humidity can be determined with humidity sensors connected to optical fibre because the experiment detects a slight change in humidity level. However, before finishing as a successful fibre optic sensor project for the agricultural industry, constructing a humidity sensor based on optical microfibre loop still needs lots of development and improvements

## 5.2 Suggestion for Future Works

The optical microfibre double loop resonator for humidity development for the industry still needs to be improved before it can be used in agriculture.

Some of the improvements include:

- i) The invention of a sustainable container for the humidity sensor.
- ii) A long-lasting optical light source capable of emitting light while maintaining a stable connection.
- iii) A research project examining various dehumidification methods in a variety of settings.
- iv) The experiment must be performed in a low-light environment to maximise the amount of reflected light at the sensor element and possibly reduce the likelihood of optical losses occurring.



## REFERENCES

- [1] Walt, D. R. (2010). Fibre optic microarrays. *Chem. Soc. Rev.*, 39(1), 38–50.  
doi:10.1039/b809339
- [2] Sakiyama, F. I. H., Lehmann, F. A., & Garrecht, H. (2019). Structural Health Monitoring of Concrete Structures using Fibre Optic Based Sensors: A Review. *Magazine of Concrete Research*, 1–45. doi:10.1680/jmacr.19.00185
- [3] Fenta, M.C., Potter, D.K. & Szanyi, J. Fibre Optic Methods of Prospecting: A Comprehensive and Modern Branch of Geophysics. *Surv Geophys* 42, 551–584 (2021). <https://doi.org/10.1007/s10712-021-09634-8>
- [4] Singh, Mandeep. (2008). Single Mode Fiber Standards: A review.
- [5] Sharma, P. (2013) Fibre Optic Communications: An overview - researchgate. Available at: [https://www.researchgate.net/profile/Prachi-Sharma-11/publication/260900908\\_Fibre\\_Optic\\_Communications\\_An\\_Overview/links/5b655c3a458515cf1d330893/Fibre-Optic-Communications-An-Overview.pdf?origin=publication\\_detail](https://www.researchgate.net/profile/Prachi-Sharma-11/publication/260900908_Fibre_Optic_Communications_An_Overview/links/5b655c3a458515cf1d330893/Fibre-Optic-Communications-An-Overview.pdf?origin=publication_detail).
- [6] M. Arumugam, —Optical Fibre Communication – An Overview| *Pramana journal of physics*, VOL. 57, Nos5 & 6, PP. 849–869, 2001.
- [7] Sánchez Martín, J. A., Bernabeu, E., Rodríguez Aramendía, A., Villalba, A., Cruzado, E., & Pardo de Santayana, M. (2014). Tapered optical fibre sensor for detection of hydrocarbon spills in seawater. 23rd International Conference on Optical Fibre Sensors. doi:10.1117/12.2058667
- [8] Patra, T. (2013) ‘Numerical Aperture of A Plastic Optical Fiber’, *International Journal of Innovations in Engineering and Technology (IJJET)*, 2(1). doi:10.21172/ijjet.

- [9] Floris, I., Adam, J. M., Calderón, P. A., & Sales, S. (2021). Fiber Optic Shape Sensors: A comprehensive review. *Optics and Lasers in Engineering*, 139, 106508. doi:10.1016/j.optlaseng.2020.106508
- [10] Ascorbe, J.; Corres, J.M.; Arregui, F.J.; Matias, I.R. Recent Developments in Fiber Optics Humidity Sensors. *Sensors* 2017, 17, 893. <https://doi.org/10.3390/s17040893>
- [11] Riza, M. A. bin, Go, Y., Harun, S. W., & Maier, R. R. J. (2020). FBG Sensors for Environmental and Biochemical Applications - A Review. *IEEE Sensors Journal*, 1–1. doi:10.1109/jsen.2020.2982446
- [12] Montero, D.S.; Vázquez, C.; Möllers, I.; Arrúe, J.; Jäger, D. A Self-Referencing Intensity Based Polymer Optical Fiber Sensor for Liquid Detection. *Sensors* 2009, 9, 6446-6455. <https://doi.org/10.3390/s90806446>
- [13] Girsang, Liliana & Napitupulu, Angelin & Simorangkir, Irmalia & Sitompul, Dahlan. (2021). Indepth Study of Single mode Optical Fibre.
- [14] Ankit Gambhir. (2013) Merits and Demerits of Optical Fiber Communication, Academia. [https://www.academia.edu/5234801/MERITS\\_AND\\_DEMERITS\\_OF\\_OPTICAL\\_FIBER\\_COMMUNICATION](https://www.academia.edu/5234801/MERITS_AND_DEMERITS_OF_OPTICAL_FIBER_COMMUNICATION)
- [15] Oleg V. Ivanov, Fibre-optic interferometer formed by a section of small-core fibre spliced between standard fibres, *Optics Communications*, Volume 282, Issue 19, 2009, ISSN 0030-4018, <https://doi.org/10.1016/j.optcom.2009.06.051>.
- [16] S. Sridhar, Suneetha Sebastian, Ajay K. Sood and Sundarajan Asokan. *Journal: IEEE Sensors Journal*, 2021, Volume 21, Number 7, Page 9171, DOI:10.1109/JSEN.2021.3054473

- [17]Zhang, L., Chen, K. S., & Yu, H.-Z. (2020). Superhydrophobic glass microfiber filter as background-free substrate for quantitative fluorometric assays. ACS Applied Materials & Interfaces. doi:10.1021/acsami.9b17432
- [18]Li, H., Huang, Y., Hou, G., Xiao, A., Chen, P., Liang, H., ... Guan, B.-O. (2019). Single-molecule detection of biomarker and localized cellular photothermal therapy using an optical microfiber with nanointerface. Science Advances, 5(12), eaax4659. doi:10.1126/sciadv.aax4659
- [19]Shahnia, S.; Ebendorff-Heidepriem, H.; Evans, D.; Afshar, S. A Fibre-Optic Platform for Sensing Nitrate Using Conducting Polymers. Sensors 2021, 21, 138. <https://doi.org/10.3390/s21010138>
- [20]Nguyen, T.H.; Sun, T.; Grattan, K.T.V. A Turn-On Fluorescence-Based Fibre Optic Sensor for the Detection of Mercury. Sensors 2019, 19, 2142. <https://doi.org/10.3390/s19092142>

## APPENDICES

### Appendix A Gantt Chart for PSM1

PROJECT ACTIVITY / TASK	WEEK													
	1	2	3	4	5	6	7	8	9	10	11	12	13	14
Project Briefing	■													
Research Project	■	■												
<b>Chapter 1</b>														
1.1 Background			■											
1.2 Problem Statement			■											
1.3 Project Objective			■											
1.4 Scope of Project			■											
<b>Chapter 2</b>														
2.1 Introduction				■										
2.2 Fibre Optic				■										
2.3 Propagation of Light Among Fibre				■										
2.4 Various Shapes and Sizes of Fibre Optic Sensor				■										
2.5 Advantages and Disadvantages of Fibre Optics					■									
2.6 Journal Comparison from Previous Work Related to the Project					■									
2.7 Summary					■									
<b>Chapter 3</b>														
3.1 Introduction						■	■							
3.2 Project Flow						■	■							
3.3 Procedure								■	■					
3.4 Summary								■	■					
Submit 1st draft										■				
<b>Chapter 4</b>														
Expected results											■			
<b>Chapter 5</b>														
Conclusion												■		
Review report													■	
Submit report													■	
Presentation														■

## Appendix B Gantt Chart for PSM2

PROJECT ACTIVITY / TASK	WEEK													
	1	2	3	4	5	6	7	8	9	10	11	12	13	14
<b>Chapter 3</b>														
3.1 Introduction														
3.2 Project Flow														
3.3 Procedure														
3.4 Summary														
Submit 1st draft														
<b>Chapter 4</b>														
4.1 Introduction														
4.2 Size of Microfibre Optical Loop Sensor														
4.3 Result and Analysis for Humidity over Time using Calcium Chloride														
4.4 Analysis of Results of the Average of Microfibre Interaction with Power over Humidity														
<b>Chapter 5</b>														
Conclusion														
Review report														
Submit report														
Presentation														

## PSM2\_turnitin check

### ORIGINALITY REPORT

<b>4%</b>	<b>3%</b>	<b>1%</b>	<b>2%</b>
SIMILARITY INDEX	INTERNET SOURCES	PUBLICATIONS	STUDENT PAPERS

### PRIMARY SOURCES

<b>1</b>	<b>ieee802.org</b> Internet Source	<b>1%</b>
<b>2</b>	<b>umpir.ump.edu.my</b> Internet Source	<b>1%</b>
<b>3</b>	<b>"Handbook of Optical Fibers", Springer Science and Business Media LLC, 2019</b> Publication	<b>&lt;1%</b>
<b>4</b>	<b>Submitted to Holy Names University</b> Student Paper	<b>&lt;1%</b>
<b>5</b>	<b>Submitted to Mahidol University</b> Student Paper	<b>&lt;1%</b>
<b>6</b>	<b>Submitted to University of Aberdeen</b> Student Paper	<b>&lt;1%</b>
<b>7</b>	<b>dspace.unza.zm</b> Internet Source	<b>&lt;1%</b>
<b>8</b>	<b>Submitted to Universiti Teknologi MARA</b> Student Paper	<b>&lt;1%</b>
<b>9</b>	<b>Submitted to University of Melbourne</b> Student Paper	<b>&lt;1%</b>

10	<a href="http://eprints.utm.my">eprints.utm.my</a> Internet Source	<1 %
11	<a href="http://www.slideshare.net">www.slideshare.net</a> Internet Source	<1 %
12	<a href="http://www.ncbi.nlm.nih.gov">www.ncbi.nlm.nih.gov</a> Internet Source	<1 %

Exclude quotes Off  
Exclude bibliography On

Exclude matches Off

